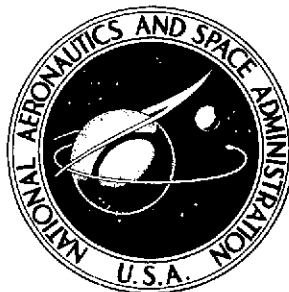
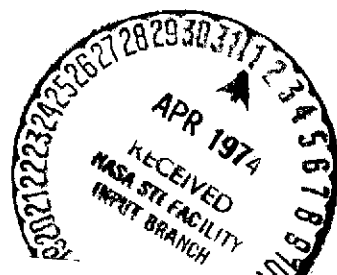


NASA TECHNICAL NOTE



NASA TN D-7407

NASA TN D-7407



(NASA-TN-D-7407) NEW TRIANGULAR AND QUADRILATERAL PLATE-BENDING FINITE ELEMENTS (NASA) 74 P HC \$3.75 CSCL 20K 75

N74-19545

Unclas
H1/32 32574

NEW TRIANGULAR AND QUADRILATERAL PLATE-BENDING FINITE ELEMENTS

by R. Narayanaswami
Langley Research Center
Hampton, Va. 23665

1. Report No. NASA TN D-7407	2. Government Accession No.	3. Recipient's Catalog No.	
4. Title and Subtitle NEW TRIANGULAR AND QUADRILATERAL PLATE-BENDING FINITE ELEMENTS		5. Report Date April 1974	6. Performing Organization Code
		8. Performing Organization Report No. L-9180	10. Work Unit No. 501-22-01-01
7. Author(s) R. Narayanaswami		11. Contract or Grant No.	
9. Performing Organization Name and Address NASA Langley Research Center Hampton, Va. 23665		13. Type of Report and Period Covered Technical Note	
		14. Sponsoring Agency Code	
12. Sponsoring Agency Name and Address National Aeronautics and Space Administration Washington, D.C. 20546		15. Supplementary Notes Author is an NRC-NASA Resident Research Associate.	
16. Abstract <p>A new nonconforming plate-bending finite element of triangular shape and associated quadrilateral elements are developed. The transverse displacement is approximated within the element by a quintic polynomial. The formulation takes into account the effects of transverse shear deformation. Results of the static and dynamic analysis of a square plate, with edges simply supported or clamped, are compared with exact solutions. Good accuracy is obtained in all calculations.</p>			
17. Key Words (Suggested by Author(s)) Plate bending Finite element Triangular element Quadrilateral element Transverse shear strains		18. Distribution Statement Unclassified - Unlimited STAR Category 32	
19. Security Classif. (of this report) Unclassified	20. Security Classif. (of this page) Unclassified	21. No. of Pages 72	22. Price* \$3.75

PRECEDING PAGE BLANK NOT FILMED

CONTENTS

SUMMARY	1
INTRODUCTION	1
SYMBOLS	3
DERIVATION OF ELEMENT PROPERTIES	6
Triangular Element	7
Element geometry	7
Displacement field	8
Elastic relationships	11
Local-global transformations	13
Stiffness matrix	15
Mass matrix	18
Consistent load vector	19
Quadrilateral Element	19
FORMULATION AND SOLUTION OF EQUATIONS	21
RESULTS AND DISCUSSION	21
Static Analysis of a Square Plate	22
Free Vibrations of a Square Plate	23
CONCLUDING REMARKS	24
APPENDIX A – DERIVATION OF RELATION BETWEEN TRANSVERSE SHEAR STRAIN AND COEFFICIENTS OF POLYNOMIAL FOR TRANSVERSE DISPLACEMENT	26
APPENDIX B – EXISTENCE OF INVERSE OF MATRIX $[R]$	35
APPENDIX C – NONZERO ELEMENTS OF MATRICES $[B_2]$ AND $[B_3]$	37
APPENDIX D – NUMERICAL INTEGRATION FORMULAS	41
APPENDIX E – STATIC CONDENSATION	42
APPENDIX F – MEDIAN PLANE FOR QUADRILATERAL ELEMENT	45
APPENDIX G – REDUCTION OF MASS MATRIX FOR QUADRILATERAL ELEMENT IN DYNAMIC ANALYSIS	47
APPENDIX H – EFFECT OF POISSON'S RATIO ON FINITE ELEMENT APPROXIMATIONS	50

REFERENCES	61
TABLES	62
FIGURES.	65

NEW TRIANGULAR AND QUADRILATERAL PLATE-BENDING FINITE ELEMENTS

By R. Narayanaswami*
Langley Research Center

SUMMARY

A new nonconforming plate-bending finite element of triangular shape is developed. The element incorporates 18 degrees of freedom: namely, the transverse displacement and rotations of the neutral surface at each vertex and at the midpoints of the sides. The formulation takes into account the effects of transverse shear deformation. The transverse displacement is approximated within the element by a quintic polynomial; thus, the bending strains vary cubically and the transverse shear strains vary quadratically.

Two associated quadrilateral elements formed by four triangular elements are also presented. The resulting internal grid points of the quadrilateral are eliminated by static condensation.

Results of the static and dynamic analysis of a square plate, with edges simply supported or clamped, are compared with exact solutions. Good accuracy is obtained in all calculations.

INTRODUCTION

The finite element method has proved to be a powerful tool for analysis of almost all problems of structural engineering. The analysis of plate-bending problems by using finite elements is important not only because it enables plates of any shape (and any support conditions) to be analyzed accurately but also because development of curved elements for shallow shell analysis depends on availability of satisfactory plate-bending elements.

Plate-bending finite elements are classified as conforming or nonconforming depending on whether or not the transverse displacement and slope normal to an edge are continuous between elements sharing the common edge. Some of the early plate-bending finite elements were developed by Clough and Tocher (ref. 1) and by Bazeley et al. (ref. 2). The conforming elements presented therein allow only a linear variation of slope normal to an edge and have been found to be overly stiff, whereas the nonconforming element given in reference 2 uses a cubic polynomial for transverse displacement and is not of very high accuracy.

*NRC-NASA Resident Research Associate.

Improvements to these elements have been made by using higher degree polynomials for transverse displacements; indeed elements of very high accuracy have been reported by Argyris et al. (ref. 3), Bell (ref. 4), and Cowper et al. (ref. 5) using quintic polynomials for the displacement field. But these elements have strains, curvatures, and/or higher order derivatives of displacements as grid point degrees of freedom which lead to an inconsistency when nonhomogeneous plates are modeled. The inconsistency is that the continuity of strains and curvatures implied by their use as degrees of freedom at grid points is violated wherever concentrated loads, abrupt changes in slope, abrupt changes in thickness, or connections to other structures occur. In short, the use of elements that assume continuity of strains and curvatures is valid only for regions where discontinuities do not occur. Further, the existence of higher order derivatives makes it difficult to impose boundary conditions and, indeed, the simple interpretation of energy derivatives as "nodal forces" disappears (ref. 6). Bell has also developed another element in reference 4, designated "T-15", which has only displacements and rotations as degrees of freedom. But element T-15 has a major drawback in that not all grid points of the element have the same degrees of freedom; consequently, it is difficult to consider connections of this element with other finite elements. Thus, the practical use of element T-15 in general purpose programs is severely limited.

The purpose of the present work is to develop a new accurate plate-bending finite element that has the advantages of the accuracy associated with a high order displacement polynomial but does not have the disadvantages just discussed and therefore will be suitable for inclusion in general purpose computer programs.

In this paper, a triangular element and associated quadrilateral elements are described in which the grid point degrees of freedom consist only of displacements and rotations; the elements use a quintic polynomial for lateral displacement. The triangular element has 18 degrees of freedom: namely, the transverse displacement and two rotations at each vertex and at the midpoints of the sides. The quadrilateral elements have 24 degrees of freedom and are formed by assembling four triangular elements.

None of the elements discussed in references 1 to 5 possess the property of transverse shear flexibility. This property has been taken into account in the present element by a procedure based on that used in NASTRAN (ref. 7). The components of transverse shear strain are quadratic functions of position. Convergence to the limiting case of zero transverse shear strain is uniform.

Two problems of plate bending are utilized to evaluate the elements, namely, the static and dynamic analysis of a square plate with edges (1) simply supported and (2) clamped. The results of calculations are compared with analytical solutions using classical plate theory and with other published finite element solutions. Good agreement is obtained with these elements for practical mesh subdivisions.

SYMBOLS

A_{11}, A_{12}, \dots	elements of matrix relating transverse shear strains to derivatives of curvatures
$\{a\}$	column vector of coefficients of transverse displacement field (generalized coordinates)
a, b, c	dimensions of triangular element in local coordinate system (fig. 1)
a_1, a_2, \dots, a_{21}	coefficients of polynomial for transverse displacement field
$[B_1], [B_2], [B_3]$	matrices relating strains and generalized displacements
b_1, b_2, \dots, b_6	coefficients of polynomial expression of γ_{xz}
$[C]$	row vector relating transverse displacement to generalized displacement
c_1, c_2, \dots, c_6	coefficients of polynomial expression of γ_{yz}
D	plate flexural rigidity, $\frac{Et^3}{12(1 - \nu^2)}$
$[D]$	matrix relating bending stress resultants and bending strains
$[D_m]$	material elastic modulus matrix
E	elastic modulus
G	shear modulus
$[G]$	matrix relating transverse shear forces and transverse shear strains
$[G_o]$	matrix relating interior grid point displacement to exterior grid point displacements of quadrilateral element
$[J]$	matrix relating transverse shear strains and transverse shear forces

$[K]$	stiffness matrix
L	length of side of plate
$[M]$	consistent mass matrix
$\{M\}$	vector of bending and twisting moments per unit length
M_x, M_y, M_{xy}	bending and twisting moments per unit length
N	number of elements per side of plate
$\{P\}$	consistent load vector
$[Q]$	matrix relating triangular element displacement vector and vector of polynomial coefficients
q	distributed loading
$[R]$	augmented matrix of $[Q]$ and constraint relations
$[S]$	matrix relating vector of polynomial coefficients and triangular element displacement vector
T	kinetic energy
$[T_1], [T_2], [T_3]$	transformation matrices
t	thickness of plate
t*	effective thickness for transverse shear
U	strain energy
$[U]$	matrix of transformation of strain components
$\{V\}$	vector of transverse shear forces per unit length

V_x, V_y	transverse shear forces per unit length
w	lateral displacement
w_c	central displacement of square plate
X, Y, Z	coordinate axes in the global system
x, y, z	coordinate axes in the local system
α	rotation of xz-plane at each grid point
β	rotation of yz-plane at each grid point
$\{\gamma\}$	vector of transverse shear strains
γ_{xz}, γ_{yz}	transverse shear strains
$\{\delta\}, \{\Delta\}$	column vector of triangular element displacement in local and global system, respectively
$\{\delta_a\}$	augmented vector of grid point displacements
$\{\delta_i\}$	triangular element displacement vector in local coordinate system at any grid point i
λ	nondimensional parameter of eigenvalues, $\frac{\rho t \omega^2 L^4}{D}$
$[\lambda]$	direction cosine matrix of quadrilateral median plane
ν	Poisson's ratio
ρ	mass density of plate material
ϕ	inclination of material orientation axis to x-axis (see fig. 1)
$\{\phi\}$	displacement vector of quadrilateral element
$\{\chi\}$	vector of bending strains

$\chi_x, \chi_y, \chi_{xy}$ bending strains

ω circular frequency of plate vibration

Subscripts:

b boundary

e element

g global

gen generalized

i interior

Superscripts:

T transpose of matrix

-1 inverse

DERIVATION OF ELEMENT PROPERTIES

In this section, the derivations of the stiffness matrix, consistent load vector, and consistent mass matrix of the elements are given. The procedure for the derivation is well documented in textbooks (see, for example, ref. 6) so that only essential details will be presented herein. The development of the triangular element follows closely that of Cowper et al. (ref. 5); the quadrilateral element is assembled from four triangular elements.

The triangular element has 18 degrees of freedom: namely, the lateral displacement w and rotations α and β at each of the six grid points. Three additional conditions are introduced by the requirement that the rotation about each edge[†] (also called edge rotation) varies cubically along each edge. This requirement establishes three constraint equations between the coefficients of the polynomial for the w displacement. These equations together with the 18 relations between the grid point degrees of freedom and the polynomial coefficients serve to evaluate uniquely the coefficients a_1 to a_{21} . The variation of deflection along any edge is a quintic polynomial in the edgewise coordinate; the six coefficients of this polynomial are uniquely determined by deflection and

[†]For the case of transverse shear strain varying within the element by a cubic or lesser degree function of position, the same three constraint equations will result by considering slope normal to each edge instead of rotation about each edge.

edgewise slope at the three grid points of the edge. Displacements are thus continuous between two elements that have a common edge. The rotation about each edge is constrained to vary cubically; however, since the rotations are defined only at three points along an edge, there is no rotation continuity between two elements that have a common edge. The element thus belongs to the class of nonconforming elements.

The quadrilateral element is formed from four triangular elements and has 24 degrees of freedom: namely, the transverse displacement and two rotations at each corner and at the midpoints of the sides. The stiffness and load matrices of the separate triangles are evaluated and added by the direct stiffness technique to form the respective matrices for the quadrilateral. The degrees of freedom associated with the internal grid points are then eliminated by static condensation.

Triangular Element

Element geometry. - Rectangular Cartesian coordinates are used in the formulation. An arbitrary triangular element is shown in figure 1. For the triangular element, X, Y, and Z are the global coordinates and x, y, and z are the local coordinates. The grid points of the element are numbered in counterclockwise direction as shown in the figure. The following relationships between the dimensions of the triangular element a, b, and c, the angle of inclination θ between the X and x axes, and the coordinates of the vertices of the element can be easily derived from figure 1:

$$\cos \theta = \frac{X_3 - X_1}{r} \quad \sin \theta = \frac{Y_3 - Y_1}{r} \quad (1)$$

$$a = (X_3 - X_5) \cos \theta - (Y_5 - Y_3) \sin \theta = \frac{(X_3 - X_5)(X_3 - X_1) + (Y_3 - Y_5)(Y_3 - Y_1)}{r} \quad (2)$$

$$b = \frac{(X_5 - X_1)(X_3 - X_1) + (Y_5 - Y_1)(Y_3 - Y_1)}{r} \quad (3)$$

$$c = \frac{(X_3 - X_1)(Y_5 - Y_1) - (Y_3 - Y_1)(X_5 - X_1)}{r} \quad (4)$$

where

$$r = \left[(X_3 - X_1)^2 + (Y_3 - Y_1)^2 \right]^{1/2} \quad (5)$$

Displacement field.- The deflection $w(x,y)$ within the triangular element is assumed to vary as a quintic polynomial in the local coordinates, that is,

$$\begin{aligned}
 w(x,y) = & a_1 + a_2x + a_3y + a_4x^2 + a_5xy + a_6y^2 + a_7x^3 + a_8x^2y + a_9xy^2 + a_{10}y^3 \\
 & + a_{11}x^4 + a_{12}x^3y + a_{13}x^2y^2 + a_{14}xy^3 + a_{15}y^4 + a_{16}x^5 + a_{17}x^4y + a_{18}x^3y^2 \\
 & + a_{19}x^2y^3 + a_{20}xy^4 + a_{21}y^5
 \end{aligned} \tag{6}$$

There are 21 independent coefficients, a_1 to a_{21} . These are evaluated by the following procedure.

The element has 18 degrees of freedom: namely, lateral displacement w in the z -direction, rotation α about the x -axis, and rotation β about the y -axis at each of the six grid points. The rotations α and β are obtained from the definitions of transverse shear strains γ_{xz} and γ_{yz} , that is,

$$\gamma_{xz} = \frac{\partial w}{\partial x} + \beta \qquad \gamma_{yz} = \frac{\partial w}{\partial y} - \alpha \tag{7}$$

It is shown in appendix A that γ_{xz} and γ_{yz} , and hence α and β , at any grid point can be expressed in terms of the coefficients a_1 to a_{21} . Thus, 18 equations relating w , α , and β at the grid points to the 21 coefficients are obtained. Three additional relations are required so that the 21 coefficients can be uniquely determined. These relations are obtained by imposing the condition that the edge rotation varies cubically along each edge. It is clear that these three constraint equations involve only the coefficients of the fifth degree terms in equation (6), since the lower degree terms satisfy the condition of cubic edge rotation automatically. Moreover, the condition depends only on the orientation of an edge. Along the edge defined by grid points 1 and 3 (where $y = 0$), the condition of cubic edge rotation requires that

$$a_{17} = 0 \tag{8}$$

Along the edge defined by grid points 1 and 5 (inclined at angle δ to the x -axis), the edge rotation r_e is given by

$$r_e = \beta \sin \delta + \alpha \cos \delta = - (5a_{16}x^4 + 4a_{17}x^3y + 3a_{18}x^2y^2 + 2a_{19}xy^3 + a_{20}y^4) \sin \delta + (a_{17}x^4 + 2a_{18}x^3y + 3a_{19}x^2y^2 + 4a_{20}xy^3 + 5a_{21}y^4) \cos \delta + \dots \quad (9)$$

where the dots indicate terms of third or lower degree. Also, along this edge,

$$x = s \cos \delta \quad y = s \sin \delta \quad (10)$$

where s is the distance along the edge and

$$\cos \delta = b / \sqrt{b^2 + c^2} \quad \sin \delta = c / \sqrt{b^2 + c^2} \quad (11)$$

By substituting x and y from equations (10) and $\cos \delta$ and $\sin \delta$ from equations (11) into equation (9) and rearranging (so that the leading term is positive), the condition for cubic variation of rotation about edge 1-5 is

$$5b^4ca_{16} + (4b^3c^2 - b^5)a_{17} + (3b^2c^3 - 2b^4c)a_{18} + (2bc^4 - 3b^3c^2)a_{19} + (c^5 - 4b^2c^3)a_{20} - 5bc^4a_{21} = 0 \quad (12)$$

Similarly, the condition for cubic variation of the rotation about the edge defined by grid points 3 and 5 (fig. 1) can be written as

$$5a^4ca_{16} + (-4a^3c^2 + a^5)a_{17} + (3a^2c^3 - 2a^4c)a_{18} + (-2ac^4 + 3a^3c^2)a_{19} + (c^5 - 4a^2c^3)a_{20} + 5ac^4a_{21} = 0 \quad (13)$$

The 18 relations between grid point displacements and the coefficients of the polynomial in equation (6) are written as

$$\{\delta\} = [Q] \{a\} \quad (14)$$

where $\{\delta\}$ is the vector of grid point displacements, $[Q]$ is the 18×21 matrix involving the coordinates of grid points substituted into the function w (eq. (6)) and the appropriate expressions of α and β derived in detail later, and $\{a\}$ is the column vector of coefficients a_1 to a_{21} . The $[Q]$ matrix is now augmented by the three constraint equations (8), (12), and (13) to form a new 21×21 matrix $[R]$ in the following equation:

$$\{\delta_a\} = [R]\{a\} \quad (15)$$

where

$$\{\delta_a\} = \begin{Bmatrix} \{\delta\} \\ 0 \\ 0 \\ 0 \end{Bmatrix}$$

For use in the evaluation of the stiffness matrix, $\{a\}$ needs to be expressed in terms of $\{\delta_a\}$ and, hence, it has to be established that the inverse of matrix $[R]$ exists. The nonsingularity of such a matrix $[R]$ for the T-15 and T-21 elements of Bell (ref. 4) follows from the completeness of the polynomials for w . Cowper et al. (ref. 5) give an explicit expression for the determinant of such a matrix and show that the matrix is nonsingular in all practical situations. In this report, a numerical experiment is described in appendix B which verifies that $[R]$ is nonsingular for all practical cases. Hence, equation (15) is inverted to give

$$\{a\} = [R]^{-1}\{\delta_a\} \quad (16)$$

This equation can also be written as

$$\{a\} = [S]\{\delta\} \quad (17)$$

where $[S]$ is a 21×18 matrix and consists of the first 18 columns of $[R]^{-1}$

From the computational standpoint, it is advantageous to substitute equation (8) into equation (6) and replace coefficients a_{18} to a_{21} by coefficients a_{17} to a_{20} , respectively. The matrix $[Q]$ then is of size 18×20 , $[R]$ becomes 20×20 , and $[S]$ becomes 20×18 . To add to the clarity of presentation, however, the complete quintic polynomial for w in equation (6) is retained throughout this report, and matrices $[Q]$, $[R]$, and $[S]$ and vector $\{a\}$ will have sizes 18×21 , 21×21 , 21×18 , and 21×1 , respectively.

Elastic relationships. - The elastic relationships are obtained from the theory of deformation for plates (ref. 8). The curvatures are defined by

$$\begin{Bmatrix} \chi_x \\ \chi_y \\ \chi_{xy} \end{Bmatrix} = \begin{Bmatrix} -\frac{\partial \beta}{\partial x} \\ \frac{\partial \alpha}{\partial y} \\ \frac{\partial \alpha}{\partial x} - \frac{\partial \beta}{\partial y} \end{Bmatrix} \quad (18)$$

Bending and twisting moments are related to curvatures by

$$\begin{Bmatrix} M_x \\ M_y \\ M_{xy} \end{Bmatrix} = [D] \begin{Bmatrix} \chi_x \\ \chi_y \\ \chi_{xy} \end{Bmatrix} \quad (19)$$

where $[D]$ is, in general, a full symmetric matrix of elastic coefficients. For a solid isotropic plate of uniform thickness t ,

$$[D] = \frac{Et^3}{12(1-\nu^2)} \begin{bmatrix} 1 & \nu & 0 \\ \nu & 1 & 0 \\ 0 & 0 & \frac{1-\nu}{2} \end{bmatrix} \quad (20)$$

For anisotropic materials, with the material orientation axis inclined at ϕ to the x-axis, the material elastic modulus matrix $[D_m]$ is transformed to the element elastic modulus matrix by

$$[D] = [U]^T [D_m] [U] \quad (21)$$

where

$$[U] = \begin{bmatrix} \cos^2 \phi & \sin^2 \phi & \cos \phi \sin \phi \\ \sin^2 \phi & \cos^2 \phi & -\cos \phi \sin \phi \\ -2 \cos \phi \sin \phi & 2 \cos \phi \sin \phi & \cos^2 \phi - \sin^2 \phi \end{bmatrix} \quad (22)$$

The positive sense of bending and twisting moments and transverse shear resultants is shown in figure 2. The moment equilibrium equations are written as

$$V_x + \frac{\partial M_x}{\partial x} + \frac{\partial M_{xy}}{\partial y} = 0 \quad (23)$$

$$V_y + \frac{\partial M_y}{\partial y} + \frac{\partial M_{xy}}{\partial x} = 0 \quad (24)$$

Transverse shear strains are related to the shear resultants by

$$\{\gamma\} = \begin{Bmatrix} \gamma_{xz} \\ \gamma_{yz} \end{Bmatrix} = [J] \begin{Bmatrix} V_x \\ V_y \end{Bmatrix} \quad (25)$$

The matrix $[J]$ is, in general, a full symmetric 2×2 matrix of elements J_{11} , J_{12} ($J_{21} = J_{12}$), and J_{22} . For a plate with isotropic transverse shear material,

$$[J] = \frac{1}{Gt^*} \begin{bmatrix} 1 & 0 \\ 0 & 1 \end{bmatrix} \quad (26)$$

where G is the shear modulus and t^* is an "effective" thickness for transverse shear. For the simple case of a plate of uniform thickness t , t^* has the value t . From appendix A, the explicit relation between the transverse shear strain and the generalized coordinates is written in matrix notation as

$$\{\gamma\} = [B_1]\{a\} \quad (27)$$

If the plate is assumed to be rigid in transverse shear, the coefficients A_{11} to A_{16} and A_{21} to A_{26} of equations (A6) are zero (since $G = \infty$) and, hence, coefficients b_1 to b_6 and c_1 to c_6 of equations (A8) and (A9) are zero. Moreover, the transverse shear strains vary linearly with G^{-1} with $\{\gamma\}$ approaching 0 as $G \rightarrow \infty$; that is, convergence to the limiting case of zero transverse shear strain is uniform.

Local-global transformations.- The displacement vector $\{\delta_i\}$ in the local coordinate system at any grid point i has three displacement components: (1) a displacement w_i in the z -direction, (2) a rotation α_i about the x -axis, and (3) a rotation β_i about the y -axis. Positive directions of the rotations are determined by the right-hand screw rule and are shown by vectors directed along the axes in figure 1. The vector $\{\delta_i\}$ is written as

$$\{\delta_i\} = \begin{Bmatrix} w_i \\ \alpha_i \\ \beta_i \end{Bmatrix} \quad (28)$$

where

$$\alpha_i = \left(\frac{\partial w}{\partial y} - \gamma_{yz} \right)_i \quad \beta_i = \left(-\frac{\partial w}{\partial x} + \gamma_{xz} \right)_i \quad (29)$$

The displacement vector in the local coordinate system is

$$\begin{aligned} \{\delta\} &= \left[\delta_1 \ \delta_2 \ \delta_3 \ \delta_4 \ \delta_5 \ \delta_6 \right]^T \\ &= \left[w_1 \ \alpha_1 \ \beta_1 \ w_2 \ \alpha_2 \ \beta_2 \ w_3 \ \alpha_3 \ \beta_3 \ w_4 \ \alpha_4 \ \beta_4 \ w_5 \ \alpha_5 \ \beta_5 \ w_6 \ \alpha_6 \ \beta_6 \right]^T \end{aligned} \quad (30)$$

The displacement components in the global system are denoted by primes (w'_i , α'_i , and β'_i); thus, the displacement vector $\{\Delta\}$ in the global coordinate system is

$$\begin{aligned} \{\Delta\} &= \left[\Delta_1 \ \Delta_2 \ \Delta_3 \ \Delta_4 \ \Delta_5 \ \Delta_6 \right]^T \\ &= \left[w'_1 \ \alpha'_1 \ \beta'_1 \ w'_2 \ \alpha'_2 \ \beta'_2 \ w'_3 \ \alpha'_3 \ \beta'_3 \ w'_4 \ \alpha'_4 \ \beta'_4 \ w'_5 \ \alpha'_5 \ \beta'_5 \ w'_6 \ \alpha'_6 \ \beta'_6 \right]^T \end{aligned} \quad (31)$$

The relationships among w , α , β , and w' , α' , β' are

$$\left. \begin{aligned} w &= w' \\ \alpha &= \alpha' \cos \theta + \beta' \sin \theta \\ \beta &= -\alpha' \sin \theta + \beta' \cos \theta \end{aligned} \right\} \quad (32)$$

where θ is the inclination between the X and x axes as shown in figure 1. The global and local displacement vectors are related by

$$\{\delta\} = [T_2] \{\Delta\} \quad (33)$$

where

$$[T_2] = \begin{bmatrix} T_1 & & & & & \\ & T_1 & & & & \\ & & T_1 & & & \\ & & & T_1 & & \\ & & & & T_1 & \\ & & & & & T_1 \end{bmatrix} \quad (34)$$

and

$$[T_1] = \begin{bmatrix} 1 & 0 & 0 \\ 0 & \cos \theta & \sin \theta \\ 0 & -\sin \theta & \cos \theta \end{bmatrix} \quad (35)$$

Stiffness matrix.- The strain energy for a plate may be written as

$$U = \frac{1}{2} \iint \left(\{M\}^T \{\chi\} + \{V\}^T \{\gamma\} \right) dx dy \quad (36)$$

where $\{M\}$ is the vector of bending and twisting moments per unit length, $\{\chi\}$ is the vector of curvatures, $\{V\}$ is the vector of transverse shear forces per unit length, and $\{\gamma\}$ is the vector of transverse shear strains. Substituting equations (19) and (25) into equation (36), and using the symmetry of $[D]$ and $[J]$ matrices, yields

$$U = \frac{1}{2} \iint \left(\{\chi\}^T [D] \{\chi\} + \{\gamma\}^T [G] \{\gamma\} \right) dx dy \quad (37)$$

where $[G] = [J]^{-1}$. The vector of curvatures $\{\chi\}$ is now rewritten as

$$\{\chi\} = \{\chi_1\} + \{\chi_2\} \quad (38)$$

where

$$\{\chi_1\} = \begin{Bmatrix} \frac{\partial^2 w}{\partial x^2} \\ \frac{\partial^2 w}{\partial y^2} \\ 2 \frac{\partial^2 w}{\partial x \partial y} \end{Bmatrix} \quad \{\chi_2\} = \begin{Bmatrix} -\frac{\partial \gamma_{xz}}{\partial x} \\ -\frac{\partial \gamma_{yz}}{\partial y} \\ -\frac{\partial \gamma_{xz}}{\partial y} - \frac{\partial \gamma_{yz}}{\partial x} \end{Bmatrix} \quad (39)$$

It follows that $\{\chi_1\}$ is the vector of curvatures in the absence of transverse shear and $\{\chi_2\}$ is the contribution of transverse shear to the vector of curvatures. The vectors $\{\chi_1\}$ and $\{\chi_2\}$ are expressed in terms of $\{a\}$, the vector of coefficients of polynomial for w (generalized coordinates), as follows:

$$\{\chi_1\} = [B_2]\{a\} \quad (40)$$

and

$$\{\chi_2\} = [B_3]\{a\} \quad (41)$$

where $[B_2]$ and $[B_3]$ are obtained by the appropriate differentiation of equations (6) and (27), respectively, and are given in appendix C. Thus,

$$\{\chi\} = \{\chi_1\} + \{\chi_2\} = \left([B_2] + [B_3] \right) \{a\} \quad (42)$$

Substituting equations (27) and (42) into (37) yields,

$$U = \frac{1}{2} \iint \{a\}^T \left(\left([B_2] + [B_3] \right)^T [D] \left([B_2] + [B_3] \right) + \left([B_1]^T [G] [B_1] \right) \right) \{a\} dx dy \quad (43)$$

With $[K]_{\text{gen}}$ denoting the generalized stiffness matrix, that is, the stiffness matrix with respect to generalized coordinates (coefficients of the displacement polynomial) $\{a\}$, the strain energy can also be expressed as

$$U = \frac{1}{2} \{a\}^T [K]_{\text{gen}} \{a\} \quad (44)$$

By comparing equations (43) and (44) and noting that $\{a\}$ is independent of x and y , the generalized stiffness matrix can be obtained as

$$[\mathbf{K}]_{\text{gen}} = \iint \left[\left([\mathbf{B}_2] + [\mathbf{B}_3] \right)^T [\mathbf{D}] \left([\mathbf{B}_2] + [\mathbf{B}_3] \right) + \left([\mathbf{B}_1] \right)^T [\mathbf{G}] [\mathbf{B}_1] \right] dx dy \quad (45)$$

The element stiffness matrix in the local coordinate system $[\mathbf{K}]_e$, that is, stiffness matrix with respect to $\{\delta\}$, is, by virtue of equation (17),

$$[\mathbf{K}]_e = [\mathbf{S}]^T [\mathbf{K}]_{\text{gen}} [\mathbf{S}] \quad (46)$$

and the element stiffness matrix in the global coordinate system $[\mathbf{K}]_g$, that is, stiffness matrix with respect to $\{\Delta\}$, is, due to equation (33),

$$[\mathbf{K}]_g = [\mathbf{T}_2]^T [\mathbf{K}]_e [\mathbf{T}_2] \quad (47)$$

The evaluation of the elements of the generalized stiffness matrix $[\mathbf{K}]_{\text{gen}}$ of equation (45) in closed form is, though straightforward, very tedious. This situation is due to the lengthy expressions involved in the triple matrix products involving matrices $[\mathbf{B}_2]$ and $[\mathbf{B}_3]$, $[\mathbf{B}_3]$ and $[\mathbf{B}_3]$, and $[\mathbf{B}_1]$ and $[\mathbf{B}_1]$. The integrations involved in equation (45) are now split into five integrals as follows:

$$\begin{aligned} [\mathbf{K}]_{\text{gen}} = & \iint [\mathbf{B}_2]^T [\mathbf{D}] [\mathbf{B}_2] dx dy + \iint [\mathbf{B}_2]^T [\mathbf{D}] [\mathbf{B}_3] dx dy + \iint [\mathbf{B}_3]^T [\mathbf{D}] [\mathbf{B}_2] dx dy \\ & + \iint [\mathbf{B}_3]^T [\mathbf{D}] [\mathbf{B}_3] dx dy + \iint [\mathbf{B}_1]^T [\mathbf{G}] [\mathbf{B}_1] dx dy \end{aligned} \quad (48)$$

The first term $\iint [\mathbf{B}_2]^T [\mathbf{D}] [\mathbf{B}_2] dx dy$ is evaluated in closed form; the other four terms are evaluated by using numerical integration. The numerical integration formulas used are listed in appendix D. If the plate is assumed to be rigid in transverse shear, the matrices $[\mathbf{B}_1]$ and $[\mathbf{B}_3]$ are null and the last four terms of equation (48) vanish.

Mass matrix.- The mass of any element is assumed to be uniformly distributed over the surface of the element. In addition, the mass is assumed to lie in the middle surface of the plate so that rotary inertia due to finite thickness is ignored.

Two different mass matrices are used: the lumped mass and the consistent mass. For the lumped mass matrix, one-sixth of the mass of the element is placed at each grid point. The consistent mass matrix is obtained from the kinetic energy under the assumption that the inertia loading does not alter the displacements at interior points. Thus, the kinetic energy may be expressed as a quadratic function of the displacements at the grid points of the element by using the geometric and elastic properties of the element and the same displacement polynomial (eq. (6)). The kinetic energy of a flat plate vibrating at radian frequency ω is

$$T = \frac{1}{2} \omega^2 \iint m w^2 dx dy \quad (49)$$

where m is mass per unit area. From equation (6),

$$w = [C] \{a\} \quad (50)$$

where

$$[C] = \begin{bmatrix} 1 & x & y & x^2 & xy & y^2 & \dots & y^5 \end{bmatrix}$$

Substituting equation (50) into equation (49) and ρt for m , where ρ is the mass density and t is the thickness, yields

$$T = \frac{1}{2} \omega^2 \rho t \iint \{a\}^T [C]^T [C] \{a\} dx dy \quad (51)$$

With $[M]_{\text{gen}}$ denoting the consistent mass matrix with respect to generalized coordinates $\{a\}$, T can also be expressed as

$$T = \frac{1}{2} \omega^2 \{a\}^T [M]_{\text{gen}} \{a\} \quad (52)$$

By comparing equations (51) and (52) and noting that $\{a\}$ is independent of x and y ,

$$[M]_{\text{gen}} = \rho t \iint [C]^T [C] dx dy \quad (53)$$

The mass matrix can be transformed to element coordinates and global coordinates by the same transformations as those used for the stiffness matrix. Thus,

$$[M]_e = [S]^T [M]_{\text{gen}} [S] \quad (54)$$

and

$$[M]_g = [T_2]^T [M]_e [T_2] \quad (55)$$

Consistent load vector.- The consistent load vector is established by imposing an arbitrary (virtual) grid point displacement and equating the external and internal work done by the various forces during that displacement. The consistent load vector with respect to generalized coordinates $\{a\}$ is found to be

$$\{P\}_{\text{gen}} = \iint [C]^T q dx dy \quad (56)$$

where q is the loading per unit area. The consistent load vector can now be transformed to element coordinates and global coordinates, respectively, by

$$\{P\}_e = [S]^T \{P\}_{\text{gen}} \quad (57)$$

$$\{P\}_g = [T_2]^T \{P\}_e \quad (58)$$

Quadrilateral Element

Two quadrilateral elements, both of which are formed from four triangular elements just described, are shown in figures 3(a) and 3(b). Each quadrilateral element has eight grid points on its edges. The first quadrilateral element, shown in figure 3(a), is designated "QUAD1." This quadrilateral element is divided first into two triangles by one diagonal (case 1) and then into two more triangles by the other diagonal (case 2). In each

case, one additional grid point is introduced at the midpoint of the diagonal; the stiffness and load matrices for the triangles are evaluated and added and the degrees of freedom associated with the internal grid point are eliminated by static condensation described in appendix E. The stiffness and load matrices of the quadrilateral element are obtained as the average of the two cases. It may be noted that, in general, grid point 9 of case 1 and case 2 need not necessarily be in the same physical location and, hence, it is necessary to use separate static condensation for each case. The second quadrilateral element, shown in figure 3(b), is designated "QUAD5." For this element, five additional grid points are introduced so that the quadrilateral is divided into four triangular elements. The eight grid points on the edges are numbered 1 to 8. Grid point 9 is located at the intersection of lines joining midpoints of opposite edges. Grid points 10 to 13 are located at the middle of the lines joining grid point 9 to each of the corners of the quadrilateral. The stiffness and load matrices for each of the four triangular elements are evaluated and added to form the respective matrices for the quadrilateral element. The degrees of freedom at internal grid points are then eliminated by static condensation.

Because the four corners of the quadrilateral need not necessarily lie in a plane and because even small deviations of any one corner from the plane of the other three corners can cause large errors when analyzing three-dimensional structures (especially when a large number of elements are used), a flat quadrilateral lying in a median plane is defined. The median plane is selected to be parallel to, and midway between, the diagonals of the quadrilateral. The adjusted flat quadrilateral is the normal projection of the given quadrilateral on the median plane. The short-line segments (of length \hat{h}) joining the corners of the original and projected quadrilateral elements are assumed to be rigid in bending and extension. This arrangement is acceptable since the short rigid extensions are only required to transfer extensional forces and bending moments to the grid points and the transformation matrix is an identity matrix. The procedure for establishing the median plane is given in appendix F. The quadrilateral element and its projection on the mean plane is shown in figure 3(c). (Grid points of the original quadrilateral are indicated by unprimed numbers and projection of grid points on the median plane are indicated by primed numbers.)

In dynamic analysis, the mass matrices of each of the constituent triangular elements of QUAD1 and QUAD5 are evaluated and added to obtain the mass matrix of the quadrilateral elements. The mass associated with the internal degrees of freedom are then eliminated by Guyan reduction (refs. 6 and 7). The procedure is explained in appendix G.

FORMULATION AND SOLUTION OF EQUATIONS

The global stiffness matrices and load vectors for the complete structure modeled by these elements are assembled from the corresponding matrices of the individual elements by standard methods (ref. 6) to form the matrix equation

$$[K]\{\Delta\} = \{P\} \quad (59)$$

Because the degrees of freedom at grid points consist of displacements and rotations, it presents no difficulty to specify the geometric boundary conditions at any irregular and/or complex boundary. After the boundary conditions are applied, the matrix equation (59) is solved by Gaussian elimination to obtain the global displacement vector $\{\Delta\}$.

RESULTS AND DISCUSSION

It is necessary for convergence that the finite element be capable of representing a state of uniform strain including rigid body motions which are states of zero strain. This criterion is satisfied for the elements presented herein. The tests performed are very simple; a plate subjected to constant curvature states was analyzed by using different finite element meshes and the finite element solution was found to coincide with the exact solution, irrespective of the subdivision of the plate. The correct representation of the rigid body motion of the element is verified by observing that the stiffness matrix for a completely free plate element contains the necessary zero eigenvalues.

The triangular and quadrilateral elements are used to solve two problems in statics and dynamics of thin isotropic plates. The formulation presented herein is capable of treating anisotropic plates and effects of transverse shear strains; however, the example problems are analyzed for the isotropic case without the effects of transverse shear strains. Such examples are chosen because the results of plate analysis by most of the other displacement model plate-bending finite elements available in the literature are presented only for such plates, and a comparison of the present elements with other available finite elements is meaningful only in such a case. In addition, the effects of transverse shear flexibility in thin plates are shown for the problems analyzed. The two problems analyzed are (1) the statics and dynamics of a square plate with edges simply supported and (2) the statics and dynamics of a square plate with edges clamped. All calculations were carried out on the CDC 6400/6600 series of computers with SCOPE operating system at the Langley Research Center. Single precision arithmetic is used throughout. A value of Poisson's ratio of 0.3 is used in all problems. The effect of variation of Poisson's ratio on the finite element approximation is shown in appendix H.

Static Analysis of a Square Plate

The arrangement of the finite elements in a quarter of the square plate is shown in figure 4. Two patterns of mesh subdivisions using the triangular elements, denoted as "P" and "Q" arrangements, are shown in figures 4(c) and (d). The number of subdivisions of the edge of the square is denoted by N . Due to symmetry, only one-quarter of the plate is analyzed. The calculated values of the deflection at the center of the plate are given in tables I and II and are compared with values obtained from the analytical solution of Timoshenko (ref. 8). These values together with those obtained from other known finite element analyses available in the literature are also compared in figures 5 to 8 in plots of deflection as a function of mesh size using a linear scale for N^{-1} .

As seen from table I, the Q arrangement is found to give better accuracy than the P arrangement for the simply supported plate for the coarsest mesh ($N = 2$); the P arrangements yield better accuracy for other mesh sizes. For the clamped plate, the P arrangements are found to be better than the Q arrangements for all mesh sizes as noted from table II. For the quadrilateral element, QUAD1 is found to be superior to QUAD5 as regards accuracy and computational efficiency.

The high accuracy achieved with the present elements (triangular and quadrilateral), even for the coarsest mesh, is evident from table I and figures 5 and 6 for the simply supported plate. For the clamped plate, the results for the coarsest grid are not as accurate as for the simply supported plate; however, as the element size is decreased, the values of deflection obtained with the present elements approach very rapidly the exact results. From a comparison of the present elements with those of Argyris et al., Bell, and Cowper et al. (refs. 3, 4, and 5) which use quintic polynomial displacement field, it is seen that all the elements are of the same order of accuracy for the simply supported plate for $\nu = 0.0$. For $\nu > 0.0$, the present elements show a variation in the value of the coefficient for central deflection; this variation is not demonstrated either in the theoretical solution (ref. 8) or in the conforming elements of references 3, 4, and 5. Nonetheless, this is characteristic of the finite element approximation with nonconforming elements. The second example of clamped plates shows a greater percentage error for these elements than those of Argyris et al. (ref. 3), Bell (ref. 9), or Cowper et al. (ref. 5) for the coarsest grid, but, for the next subdivision of $N = 4$, the value of maximum deflection differs from the exact by less than 4.5 percent for concentrated load and 3 percent for uniformly distributed loading. The accuracy attainable by the present elements for practical subdivisions is quite satisfactory. The calculated deflection along a center line of a square plate for the simply supported plate for a central point load (since this case represents one of the severest test cases for finite element method) is plotted in figure 9. Good agreement is seen in both cases with the exact solution.

The results shown in tables I and II and in figures 5 to 9 were obtained for the present elements without taking into account the effects of transverse shear deformation so as to obtain meaningful comparisons with other finite elements. The values of the coefficients for central deflection with transverse shear effects are calculated for a square plate with $L/t = 96$ and are given in table III. For the P arrangement of the example shown, the value of maximum deflection varies by 0.1138 percent and 0.2632 percent for central concentrated load and by 0.0283 percent and 0.1335 percent for uniformly distributed loads (for simply supported and clamped edge conditions of the plate, respectively). These effects are so small that the question may be posed whether it is worthwhile to consider them in the stiffness formulation. The answer to this question lies in the fact that the effects of transverse shear are negligibly small for thin isotropic plates (thin isotropic plates were chosen here for reasons cited earlier) but are significant for moderately thick or thick plates, anisotropic plates, and sandwich shells consisting of soft core and stiff plates. For all such cases, the present elements have a decided advantage over most other displacement formulation plate-bending elements now available in the literature.

Free Vibrations of a Square Plate

The natural frequencies of a square plate were determined by using the triangular and quadrilateral elements. The nondimensional eigenvalues are defined as

$$\lambda = \frac{\rho t \omega^2 L^4}{D} \quad (60)$$

where

ρ mass density

t thickness of plate

ω circular frequency

L length of side of square plate

$D = \frac{Et^3}{12(1 - \nu^2)}$ the flexural rigidity of the plate

The exact eigenvalues for the simply supported plate are given by

$$\lambda = (r^2 + s^2)^2 \pi^4 \quad (61)$$

where (r,s) refers to the number of half-waves parallel to the edge directions.

The lowest six eigenvalues obtained by using the present elements and the exact results are shown in table IV. The eigenvalue problems are solved by using a Jacobi routine that produces the complete set of eigenvalues and eigenvectors. A consistent mass matrix is used for all calculations. It is seen that the lowest eigenvalue is calculated to within 3 percent of the exact value for the coarsest mesh. Good agreement is obtained for higher eigenvalues as well. For the examples of $(r + s)$ or $(r - s)$ even, λ_{rs} is not equal to λ_{sr} when triangular elements are used, even though this equality should be the case due to the symmetry of the configuration. However, for quadrilateral elements there is no such discrepancy. A comparison of the lowest eigenvalue for the simply supported plate using the present elements and other finite element solutions is given in table V. The present elements are more accurate than the ACM or CFQ elements (refs. 1 and 10) but slightly less accurate than that of Cowper et al. (ref. 5).

The results of calculations for a square plate with clamped edges are shown in table VI. No exact solution is available for this case and, therefore, the present values are compared with the upper and lower bound values given in reference 5. Reasonable agreement is observed although the accuracy is not as good as that for the simply supported plate.

CONCLUDING REMARKS

A new triangular plate-bending finite element using a quintic polynomial for transverse displacement is described. The element has only displacements and rotations as grid point degrees of freedom and thus avoids certain ambiguities associated with the second and higher order derivatives of displacements as degrees of freedom. Two associated quadrilateral elements are also described which are assembled from the basic triangular element. Sample calculations for the static and dynamic analysis of plates were performed and the results were compared with analytical solutions using classical plate theory and with other published finite element solutions. Good agreement was obtained with these elements for practical mesh subdivisions.

The effect of transverse shear deformations is included in the element formulation. Convergence to the case of zero transverse shear strain is uniform. The present elements are expected to give better approximations than most displacement model plate-bending elements for solving problems where transverse shear effects are significant.

These elements are ideally suited for inclusion into general purpose computer programs because of (1) simplicity of formulation, (2) use of only displacements and rotations as grid point degrees of freedom, (3) high accuracy for practical mesh subdivisions, and (4) inclusion of transverse shear flexibility in the element properties.

Langley Research Center,
National Aeronautics and Space Administration,
Hampton, Va., January 25, 1974.

APPENDIX A

DERIVATION OF RELATION BETWEEN TRANSVERSE SHEAR STRAIN AND COEFFICIENTS OF POLYNOMIAL FOR TRANSVERSE DISPLACEMENT

From equations (23), (24), and (25), it follows that

$$\left. \begin{aligned} \gamma_{xz} &= -J_{11} \left[\frac{\partial M_x}{\partial x} + \frac{\partial M_{xy}}{\partial y} \right] - J_{12} \left[\frac{\partial M_y}{\partial y} + \frac{\partial M_{xy}}{\partial x} \right] \\ \gamma_{yz} &= -J_{12} \left[\frac{\partial M_x}{\partial x} + \frac{\partial M_{xy}}{\partial y} \right] - J_{22} \left[\frac{\partial M_y}{\partial y} + \frac{\partial M_{xy}}{\partial x} \right] \end{aligned} \right\} \quad (A1)$$

Performing the partial differentiation with respect to x and y on equation (19), with subscripts on D denoting the elements of $[D]$, results in

$$\left. \begin{aligned} \frac{\partial M_x}{\partial x} &= D_{11} \frac{\partial \chi_x}{\partial x} + D_{12} \frac{\partial \chi_y}{\partial x} + D_{13} \frac{\partial \chi_{xy}}{\partial x} \\ \frac{\partial M_y}{\partial y} &= D_{12} \frac{\partial \chi_x}{\partial y} + D_{22} \frac{\partial \chi_y}{\partial y} + D_{23} \frac{\partial \chi_{xy}}{\partial y} \\ \frac{\partial M_{xy}}{\partial x} &= D_{13} \frac{\partial \chi_x}{\partial x} + D_{23} \frac{\partial \chi_y}{\partial x} + D_{33} \frac{\partial \chi_{xy}}{\partial x} \\ \frac{\partial M_{xy}}{\partial y} &= D_{13} \frac{\partial \chi_x}{\partial y} + D_{23} \frac{\partial \chi_y}{\partial y} + D_{33} \frac{\partial \chi_{xy}}{\partial y} \end{aligned} \right\} \quad (A2)$$

where the symmetry of the $[D]$ matrix has been used. By substituting equations (A2) into equations (A1),

APPENDIX A

$$\begin{aligned} \gamma_{xz} = & -J_{11} \left[D_{11} \frac{\partial \chi_x}{\partial x} + D_{12} \frac{\partial \chi_y}{\partial x} + D_{13} \frac{\partial \chi_{xy}}{\partial x} + D_{13} \frac{\partial \chi_x}{\partial y} + D_{23} \frac{\partial \chi_y}{\partial y} + D_{33} \frac{\partial \chi_{xy}}{\partial y} \right] \\ & -J_{12} \left[D_{12} \frac{\partial \chi_x}{\partial y} + D_{22} \frac{\partial \chi_y}{\partial y} + D_{23} \frac{\partial \chi_{xy}}{\partial y} + D_{13} \frac{\partial \chi_x}{\partial x} + D_{23} \frac{\partial \chi_y}{\partial x} + D_{33} \frac{\partial \chi_{xy}}{\partial x} \right] \end{aligned} \quad (A3)$$

and

$$\begin{aligned} \gamma_{yz} = & -J_{12} \left[D_{11} \frac{\partial \chi_x}{\partial x} + D_{12} \frac{\partial \chi_y}{\partial x} + D_{13} \frac{\partial \chi_{xy}}{\partial x} + D_{13} \frac{\partial \chi_x}{\partial y} + D_{23} \frac{\partial \chi_y}{\partial y} + D_{33} \frac{\partial \chi_{xy}}{\partial y} \right] \\ & -J_{22} \left[D_{12} \frac{\partial \chi_x}{\partial y} + D_{22} \frac{\partial \chi_y}{\partial y} + D_{23} \frac{\partial \chi_{xy}}{\partial y} + D_{13} \frac{\partial \chi_x}{\partial x} + D_{23} \frac{\partial \chi_y}{\partial x} + D_{33} \frac{\partial \chi_{xy}}{\partial x} \right] \end{aligned} \quad (A4)$$

Rearranging and writing equations (A3) and (A4) in matrix notation yields

$$\begin{Bmatrix} \gamma_{xz} \\ \gamma_{yz} \end{Bmatrix} = \begin{bmatrix} A_{11} & A_{12} & A_{13} & A_{14} & A_{15} & A_{16} \\ A_{21} & A_{22} & A_{23} & A_{24} & A_{25} & A_{26} \end{bmatrix} \begin{Bmatrix} \chi_{x,x} \\ \chi_{y,x} \\ \chi_{xy,x} \\ \chi_{x,y} \\ \chi_{y,y} \\ \chi_{xy,y} \end{Bmatrix} \quad (A5)$$

where a comma in the subscript denotes partial differentiation and where

$$A_{11} = -(J_{11}D_{11} + J_{12}D_{13}) \quad (A6a)$$

$$A_{12} = -(J_{11}D_{12} + J_{12}D_{23}) \quad (A6b)$$

$$A_{13} = -(J_{11}D_{13} + J_{12}D_{33}) \quad (A6c)$$

APPENDIX A

$$A_{14} = -(J_{11}D_{13} + J_{12}D_{12}) \quad (A6d)$$

$$A_{15} = -(J_{11}D_{23} + J_{12}D_{22}) \quad (A6e)$$

$$A_{16} = -(J_{11}D_{33} + J_{12}D_{23}) \quad (A6f)$$

$$A_{21} = -(J_{12}D_{11} + J_{22}D_{13}) \quad (A6g)$$

$$A_{22} = -(J_{12}D_{12} + J_{22}D_{23}) \quad (A6h)$$

$$A_{23} = -(J_{12}D_{13} + J_{22}D_{33}) \quad (A6i)$$

$$A_{24} = -(J_{12}D_{13} + J_{22}D_{12}) \quad (A6j)$$

$$A_{25} = -(J_{12}D_{23} + J_{22}D_{22}) \quad (A6k)$$

$$A_{26} = -(J_{12}D_{33} + J_{22}D_{23}) \quad (A6l)$$

From equations (7) and (18), it follows that

$$\left. \begin{aligned} \chi_x &= -\frac{\partial\beta}{\partial x} = \frac{\partial^2 w}{\partial x^2} - \frac{\partial\gamma_{xz}}{\partial x} \\ \chi_y &= \frac{\partial\alpha}{\partial y} = \frac{\partial^2 w}{\partial y^2} - \frac{\partial\gamma_{yz}}{\partial y} \\ \chi_{xy} &= \frac{\partial\alpha}{\partial x} - \frac{\partial\beta}{\partial y} = 2\frac{\partial^2 w}{\partial x \partial y} - \frac{\partial\gamma_{xz}}{\partial y} - \frac{\partial\gamma_{yz}}{\partial x} \end{aligned} \right\} \quad (A7)$$

Shear forces (and hence shear strains) are proportional to the third derivatives of the displacements. Since the displacement within the element is assumed to vary as a quintic polynomial, shear strains are expressed by a quadratic polynomial as follows:

$$\gamma_{xz} = b_1 + b_2x + b_3y + b_4x^2 + b_5xy + b_6y^2 \quad (A8)$$

APPENDIX A

$$\gamma_{yz} = c_1 + c_2x + c_3y + c_4x^2 + c_5xy + c_6y^2 \quad (A9)$$

The task now is to express the unknown coefficients b_1 to b_6 and c_1 to c_6 in terms of the generalized coordinates a_1 to a_{21} . Performing the differentiations on χ_x , χ_y , and χ_{xy} and substituting w , γ_{xz} , and γ_{yz} from equations (6), (A8), and (A9) into equations (A7) results in

$$\chi_{x,x} = \frac{\partial^3 w}{\partial x^3} - \frac{\partial^2 \gamma_{xz}}{\partial x^2} = 6a_7 + 24a_{11}x + 6a_{12}y + 60a_{16}x^2 + 24a_{17}xy + 6a_{18}y^2 - 2b_4 \quad (A10)$$

$$\chi_{y,x} = \frac{\partial^3 w}{\partial x \partial y^2} - \frac{\partial^2 \gamma_{yz}}{\partial x \partial y} = 2a_9 + 4a_{13}x + 6a_{14}y + 6a_{18}x^2 + 12a_{19}xy + 12a_{20}y^2 - c_5 \quad (A11)$$

$$\begin{aligned} \chi_{xy,x} &= 2 \frac{\partial^3 w}{\partial x^2 \partial y} - \frac{\partial^2 \gamma_{xz}}{\partial x \partial y} - \frac{\partial^2 \gamma_{yz}}{\partial x^2} \\ &= 4a_8 + 12a_{12}x + 8a_{13}y + 24a_{17}x^2 + 24a_{18}xy + 12a_{19}y^2 - b_5 - 2c_4 \end{aligned} \quad (A12)$$

$$\chi_{x,y} = \frac{\partial^3 w}{\partial x^2 \partial y} - \frac{\partial^2 \gamma_{xz}}{\partial x \partial y} = 2a_8 + 6a_{12}x + 4a_{13}y + 12a_{17}x^2 + 12a_{18}xy + 6a_{19}y^2 - b_5 \quad (A13)$$

$$\chi_{y,y} = \frac{\partial^3 w}{\partial y^3} - \frac{\partial^2 \gamma_{yz}}{\partial y^2} = 6a_{10} + 6a_{14}x + 24a_{15}y + 6a_{19}x^2 + 24a_{20}xy + 60a_{21}y^2 - 2c_6 \quad (A14)$$

$$\begin{aligned} \chi_{xy,y} &= 2 \frac{\partial^2 w}{\partial x \partial y^2} - \frac{\partial^2 \gamma_{xz}}{\partial y^2} - \frac{\partial^2 \gamma_{yz}}{\partial x \partial y} \\ &= 4a_9 + 8a_{13}x + 12a_{14}y + 12a_{18}x^2 + 24a_{19}xy + 24a_{20}y^2 - 2b_6 - c_5 \end{aligned} \quad (A15)$$

APPENDIX A

By substituting equations (A8) to (A15) into equations (A5), the following equations are obtained:

$$\begin{aligned}
 b_1 + b_2x + b_3y + b_4x^2 + b_5xy + b_6y^2 = & A_{11}(6a_7 + 24a_{11}x + 6a_{12}y + 60a_{16}x^2 + 24a_{17}xy \\
 & + 6a_{18}y^2 - 2b_4) + A_{12}(2a_9 + 4a_{13}x + 6a_{14}y \\
 & + 6a_{18}x^2 + 12a_{19}xy + 12a_{20}y^2 - c_5) + A_{13}(4a_8 \\
 & + 12a_{12}x + 8a_{13}y + 24a_{17}x^2 + 24a_{18}xy + 12a_{19}y^2 \\
 & - b_5 - 2c_4) + A_{14}(2a_8 + 6a_{12}x + 4a_{13}y + 12a_{17}x^2 \\
 & + 12a_{18}xy + 6a_{19}y^2 - b_5) + A_{15}(6a_{10} + 6a_{14}x \\
 & + 24a_{15}y + 6a_{19}x^2 + 24a_{20}xy + 60a_{21}y^2 - 2c_6) \\
 & + A_{16}(4a_9 + 8a_{13}x + 12a_{14}y + 12a_{18}x^2 + 24a_{19}xy \\
 & + 24a_{20}y^2 - 2b_6 - c_5) \tag{A16}
 \end{aligned}$$

$$\begin{aligned}
 c_1 + c_2x + c_3y + c_4x^2 + c_5xy + c_6y^2 = & A_{21}(6a_7 + 24a_{11}x + 6a_{12}y + 60a_{16}x^2 + 24a_{17}xy \\
 & + 6a_{18}y^2 - 2b_4) + A_{22}(2a_9 + 4a_{13}x + 6a_{14}y \\
 & + 6a_{18}x^2 + 12a_{19}xy + 12a_{20}y^2 - c_5) + A_{23}(4a_8 \\
 & + 12a_{12}x + 8a_{13}y + 24a_{17}x^2 + 24a_{18}xy + 12a_{19}y^2 \\
 & - b_5 - 2c_4) + A_{24}(2a_8 + 6a_{12}x + 4a_{13}y + 12a_{17}x^2 \\
 & + 12a_{18}xy + 6a_{19}y^2 - b_5) + A_{25}(6a_{10} + 6a_{14}x \\
 & + 24a_{15}y + 6a_{19}x^2 + 24a_{20}xy + 60a_{21}y^2 - 2c_6) \\
 & + A_{26}(4a_9 + 8a_{13}x + 12a_{14}y + 12a_{18}x^2 + 24a_{19}xy \\
 & + 24a_{20}y^2 - 2b_6 - c_5) \tag{A17}
 \end{aligned}$$

APPENDIX A

By comparing coefficients of like powers in x , y , x^2 , xy , and y^2 and constants of equations (A16) and (A17), the coefficients b_1 to b_6 and c_1 to c_6 can be expressed in terms of the generalized coordinates a_1 to a_{21} . Thus,

$$\begin{aligned}
 b_2 &= 24A_{11}a_{11} + 6(A_{14} + 2A_{13})a_{12} + 4(A_{12} + 2A_{16})a_{13} + 6A_{15}a_{14} \\
 b_3 &= 6A_{11}a_{12} + 4(A_{14} + 2A_{13})a_{13} + 6(A_{12} + 2A_{16})a_{14} + 24A_{15}a_{15} \\
 b_4 &= 60A_{11}a_{16} + 12(A_{14} + 2A_{13})a_{17} + 6(A_{12} + 2A_{16})a_{18} + 6A_{15}a_{19} \\
 b_5 &= 24A_{11}a_{17} + 12(A_{14} + 2A_{13})a_{18} + 12(A_{12} + 2A_{16})a_{19} + 24A_{15}a_{20} \\
 b_6 &= 6A_{11}a_{18} + 6(A_{14} + 2A_{13})a_{19} + 12(A_{12} + 2A_{16})a_{20} + 60A_{15}a_{21} \\
 b_1 &= 6A_{11}a_7 + 2(A_{14} + 2A_{13})a_8 + 2(A_{12} + 2A_{16})a_9 + 6A_{15}a_{10} - 2A_{11}b_4 - (A_{13} \\
 &\quad + A_{14})b_5 - 2A_{16}b_6 - 2A_{13}c_4 - (A_{12} + A_{16})c_5 - 2A_{15}c_6
 \end{aligned}
 \tag{A18}$$

$$\begin{aligned}
 c_2 &= 24A_{21}a_{11} + 6(A_{24} + 2A_{23})a_{12} + 4(A_{22} + 2A_{26})a_{13} + 6A_{25}a_{14} \\
 c_3 &= 6A_{21}a_{12} + 4(A_{24} + 2A_{23})a_{13} + 6(A_{22} + 2A_{26})a_{14} + 24A_{25}a_{15} \\
 c_4 &= 60A_{21}a_{16} + 12(A_{24} + 2A_{23})a_{17} + 6(A_{22} + 2A_{26})a_{18} + 6A_{25}a_{19} \\
 c_5 &= 24A_{21}a_{17} + 12(A_{24} + 2A_{23})a_{18} + 12(A_{22} + 2A_{26})a_{19} + 24A_{25}a_{20} \\
 c_6 &= 6A_{21}a_{18} + 6(A_{24} + 2A_{23})a_{19} + 12(A_{22} + 2A_{26})a_{20} + 60A_{25}a_{21} \\
 c_1 &= 6A_{21}a_7 + 2(A_{24} + 2A_{23})a_8 + 2(A_{22} + 2A_{26})a_9 + 6A_{25}a_{10} - 2A_{21}b_4 - (A_{23} \\
 &\quad + A_{24})b_5 - 2A_{26}b_6 - 2A_{23}c_4 - (A_{22} + A_{26})c_5 - 2A_{25}c_6
 \end{aligned}
 \tag{A19}$$

APPENDIX A

If equations (A18) and (A19) are substituted into equations (A8) and (A9), the explicit relation between the transverse shear strain and the generalized coordinates (i.e., coefficients of the displacement polynomial) can be obtained in matrix notation as

$$\{\gamma\} = [B_1]\{a\} \quad (A20)$$

where $[B_1]$ is a 2×21 matrix whose nonzero elements are as follows:

$$B_1(1,7) = 6A_{11}$$

$$B_1(1,8) = 2A_{31}$$

$$B_1(1,9) = 2A_{32}$$

$$B_1(1,10) = 6A_{15}$$

$$B_1(1,11) = 24A_{11}x$$

$$B_1(1,12) = 6(A_{31}x + A_{11}y)$$

$$B_1(1,13) = 4(A_{32}x + A_{31}y)$$

$$B_1(1,14) = 6(A_{15}x + A_{32}y)$$

$$B_1(1,15) = 24A_{15}y$$

$$B_1(1,16) = -120(A_{11}^2 + A_{13}A_{21} - 0.5A_{11}x^2)$$

$$B_1(1,17) = -24\left[A_{11}(A_{31} + A_{38}) + A_{13}A_{33} + A_{21}A_{39} - 0.5A_{31}x^2 - A_{11}xy\right]$$

$$B_1(1,18) = -12\left(A_{11}A_{32} + A_{13}A_{34} + A_{38}A_{31} + A_{39}A_{33} + A_{11}A_{16} + A_{15}A_{21} - 0.5A_{32}x^2 - A_{31}xy - 0.5A_{11}y^2\right)$$

APPENDIX A

$$B_1(1,19) = -12(A_{11}A_{15} + A_{13}A_{25} + A_{38}A_{32} + A_{39}A_{34} + A_{16}A_{31} + A_{15}A_{33} \\ - 0.5A_{15}x^2 - A_{32}xy - 0.5A_{31}y^2)$$

$$B_1(1,20) = -24(A_{15}A_{38} + A_{25}A_{39} + A_{16}A_{32} + A_{15}A_{34} - A_{15}xy - 0.5A_{32}y^2)$$

$$B_1(1,21) = -120(A_{15}A_{16} + A_{15}A_{25} - 0.5A_{15}y^2)$$

$$B_1(2,7) = 6A_{21}$$

$$B_1(2,8) = 2A_{33}$$

$$B_1(2,9) = 2A_{34}$$

$$B_1(2,10) = 6A_{25}$$

$$B_1(2,11) = 24A_{21}x$$

$$B_1(2,12) = 6(A_{33}x + A_{21}y)$$

$$B_1(2,13) = 4(A_{34}x + A_{33}y)$$

$$B_1(2,14) = 6(A_{25}x + A_{34}y)$$

$$B_1(2,15) = 24A_{25}y$$

$$B_1(2,16) = -120(A_{11}A_{21} + A_{23}A_{21} - 0.5A_{21}x^2)$$

$$B_1(2,17) = -24(A_{21}A_{31} + A_{11}A_{40} + A_{23}A_{33} + A_{21}A_{34} - 0.5A_{33}x^2 - A_{21}xy)$$

$$B_1(2,18) = -12(A_{21}A_{32} + A_{23}A_{34} + A_{40}A_{31} + A_{41}A_{33} + A_{26}A_{11} + A_{25}A_{21} \\ - 0.5A_{34}x^2 - A_{33}xy - 0.5A_{21}y^2)$$

APPENDIX A

$$B_1(2,19) = -12(A_{21}A_{15} + A_{23}A_{25} + A_{40}A_{32} + A_{41}A_{34} + A_{26}A_{31} + A_{25}A_{33} - 0.5A_{25}x^2 - A_{34}xy - 0.5A_{33}y^2)$$

$$B_1(2,20) = -24(A_{15}A_{40} + A_{25}A_{41} + A_{26}A_{32} + A_{25}A_{34} - A_{25}xy - 0.5A_{34}y^2)$$

$$B_1(2,21) = -120(A_{15}A_{26} + A_{25}^2 - 0.5A_{25}y^2)$$

where A_{11} , A_{12} , A_{13} , A_{14} , A_{15} , A_{16} , A_{21} , A_{22} , A_{23} , A_{24} , A_{25} , and A_{26} are as defined in equations (A6) and

$$\left. \begin{aligned} A_{31} &= A_{14} + 2A_{13} \\ A_{32} &= A_{12} + 2A_{16} \\ A_{33} &= A_{24} + 2A_{23} \\ A_{34} &= A_{22} + 2A_{26} \\ A_{35} &= A_{33} + A_{11} \\ A_{36} &= A_{34} + A_{31} \\ A_{37} &= A_{25} + A_{32} \\ A_{38} &= A_{13} + A_{14} \\ A_{39} &= A_{12} + A_{16} \\ A_{40} &= A_{23} + A_{24} \\ A_{41} &= A_{22} + A_{26} \end{aligned} \right\} \quad (A21)$$

APPENDIX B

EXISTENCE OF INVERSE OF MATRIX $[R]$

The details of the numerical experiment performed to verify the existence of the inverse of matrix $[R]$ (see eq. (15) and the paragraph that follows on p. 10) are given in this appendix. Three cases of the triangular element are considered and for each case the inverse of matrix $[R]$ was evaluated with and without transverse shear effects. Since it is not possible to consider the infinite combinations of geometric and material properties that yield varying transverse shear effects, a practical case of significant transverse shear and the case with no transverse shear are considered. Any intermediate case of transverse shear effect will produce results between the two extreme situations analyzed.

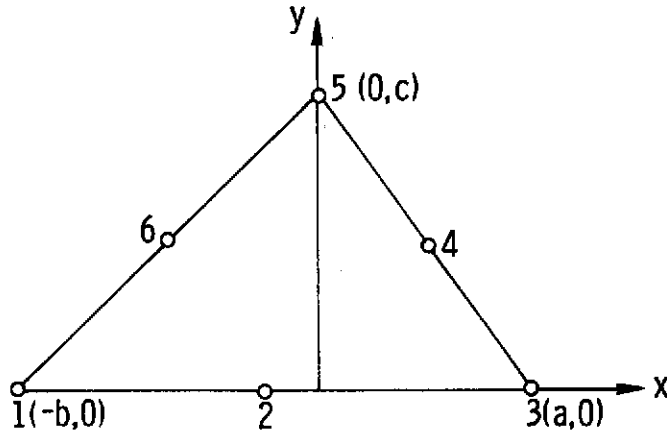
The three cases of the triangular element are shown in figures B1(a) to B1(c). Figure B1(a) shows a triangle with three acute angles. Figure B1(b) shows the triangle with two acute angles at grid points 3 and 5 and an obtuse angle at grid point 1. Figure B1(c) shows the triangle with two acute angles at grid points 1 and 5 and an obtuse angle at grid point 3.

A total of 300 triangles, about 100 in each case, with varying values of the dimension of the triangle a , b , and c were analyzed. The $[R]$ matrix was formed, and the determinant and inverse of the matrix $[R]$ were evaluated. Single-precision arithmetic was used in the calculations. The determinant of $[R]$ was nonzero in all examples analyzed. For small values of a , b , and c (say, $a = 0.1$, $b = 0.1$, and $c = 0.1$), the determinant of $[R]$ was very small; however, no instability was observed in evaluating the inverse. (The elements of $[R]^{-1}$ were observed for any unbounded growth of the numbers as the value of the determinant of $[R]$ became smaller and smaller. The maximum value of any element of $[R]^{-1}$ for the problem with the smallest value of the determinant of $[R]$ was of the order of 10^3 . The matrix $[R]^{-1}$ was very stable for all the problems investigated.)

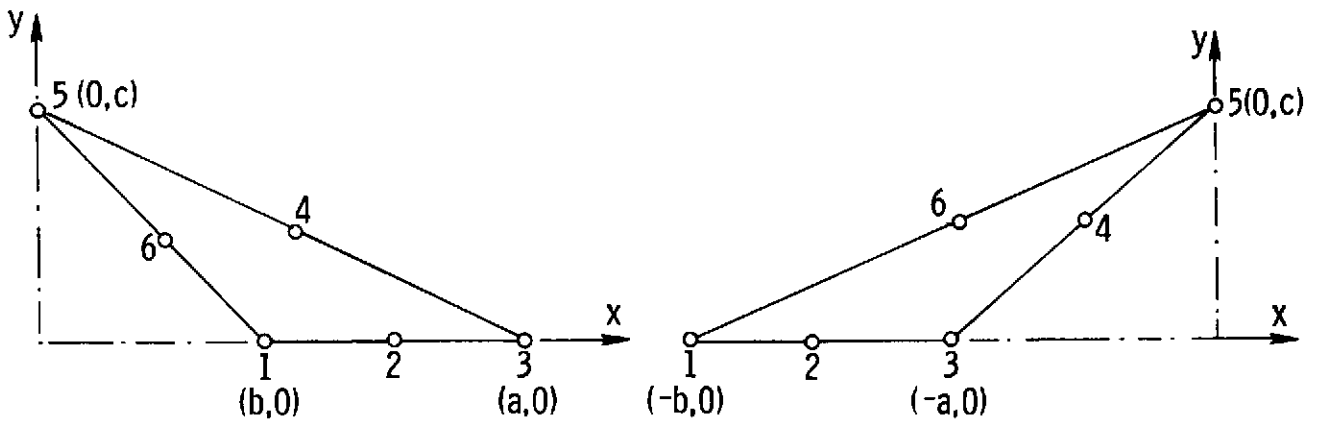
The same 300 problems were used to evaluate the inverse of $[R]$ for the case with significant transverse shear strains. In general, the effect of the transverse shear strains

APPENDIX B

was to increase the value of the determinant of $[R]$ and, hence, even for problems with small values of a , b , and c of the triangle, the determinant of $[R]$ was considerably higher. No instability was noticed in any of the examples analyzed.



(a) Acute angles at grid points 1, 3, and 5.



(b) Obtuse angle at grid point 1.

(c) Obtuse angle at grid point 3.

Figure B1.- Triangular element shapes.

APPENDIX C

NONZERO ELEMENTS OF MATRICES $[B_2]$ AND $[B_3]$

The nonzero elements of matrix $[B_2]$ (see eq. (40)) are as follows:

$$B_2(1,4) = 2$$

$$B_2(1,7) = 6x$$

$$B_2(1,8) = 2y$$

$$B_2(1,11) = 12x^2$$

$$B_2(1,12) = 6xy$$

$$B_2(1,13) = 2y^2$$

$$B_2(1,16) = 20x^3$$

$$B_2(1,17) = 12x^2y$$

$$B_2(1,18) = 6xy^2$$

$$B_2(1,19) = 2y^3$$

$$B_2(2,6) = 2$$

$$B_2(2,9) = 2x$$

$$B_2(2,10) = 6y$$

$$B_2(2,13) = 2x^2$$

APPENDIX C

$$B_2(2,14) = 6xy$$

$$B_2(2,15) = 12y^2$$

$$B_2(2,18) = 2x^3$$

$$B_2(2,19) = 6x^2y$$

$$B_2(2,20) = 12xy^2$$

$$B_2(2,21) = 20y^3$$

$$B_2(3,5) = 2$$

$$B_2(3,8) = 4x$$

$$B_2(3,9) = 4y$$

$$B_2(3,12) = 6x^2$$

$$B_2(3,13) = 8xy$$

$$B_2(3,14) = 6y^2$$

$$B_2(3,17) = 8x^3$$

$$B_2(3,18) = 12x^2y$$

$$B_2(3,19) = 12xy^2$$

$$B_2(3,20) = 8y^3$$

APPENDIX C

The nonzero elements of matrix $[B_3]$ (see eq. (41)) are as follows:

$$B_3(1,11) = -24A_{11}$$

$$B_3(1,12) = -6A_{31}$$

$$B_3(1,13) = -4A_{32}$$

$$B_3(1,14) = -6A_{15}$$

$$B_3(1,16) = -120A_{11}x$$

$$B_3(1,17) = -24(A_{31}x + A_{11}y)$$

$$B_3(1,18) = -12(A_{32}x + A_{31}y)$$

$$B_3(1,19) = -12(A_{15}x + A_{32}y)$$

$$B_3(1,20) = -24A_{15}y$$

$$B_3(2,12) = -6A_{21}$$

$$B_3(2,13) = -4A_{33}$$

$$B_3(2,14) = -6A_{34}$$

$$B_3(2,15) = -24A_{25}$$

$$B_3(2,17) = -24A_{21}x$$

$$B_3(2,18) = -12(A_{33}x + A_{21}y)$$

$$B_3(2,19) = -12(A_{34}x + A_{33}y)$$

APPENDIX C

$$B_3(2,20) = -24(A_{25}x + A_{34}y)$$

$$B_3(2,21) = -120A_{25}y$$

$$B_3(3,11) = -24A_{21}$$

$$B_3(3,12) = -6(A_{11} + A_{33})$$

$$B_3(3,13) = -4(A_{31} + A_{34})$$

$$B_3(3,14) = -6(A_{32} + A_{25})$$

$$B_3(3,15) = -24A_{15}$$

$$B_3(3,16) = -120A_{21}x$$

$$B_3(3,17) = -24[(A_{11} + A_{33})x + A_{21}y]$$

$$B_3(3,18) = -12[(A_{34} + A_{31})x + (A_{33} + A_{11})y]$$

$$B_3(3,19) = -12[(A_{25} + A_{32})x + (A_{34} + A_{31})y]$$

$$B_3(3,20) = -24[A_{15}x + (A_{32} + A_{25})y]$$

$$B_3(3,21) = -120A_{15}y$$

where $A_{11}, A_{12}, \dots, A_{34}$ are as given in equations (A6) and (A21).

APPENDIX D

NUMERICAL INTEGRATION FORMULAS

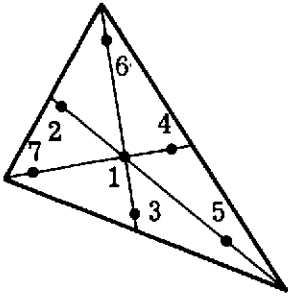
For a triangle, the integrals of the form

$$I = \int_0^1 \int_0^{1-L_1} f(L_1 L_2 L_3) dL_1 dL_2 \quad (D1)$$

can be integrated by using a seven-point numerical integration which can exactly integrate functions up to and including quintic order. The value of the integral is given by

$$I = \sum_{k=1}^7 W_k f_k(L_1, L_2, L_3) \quad (D2)$$

where the points and the weighting factors are as follows:



Point	Triangular coordinates, L_1, L_2, L_3	Weight, $2W_k$
1	$1/3, 1/3, 1/3$	0.225
2	$\alpha_1, \beta_1, \beta_1$	0.13239415
3	$\beta_1, \alpha_1, \beta_1$	
4	$\beta_1, \beta_1, \alpha_1$	
5	$\alpha_2, \beta_2, \beta_2$	
6	$\beta_2, \alpha_2, \beta_2$	0.12593918
7	$\beta_2, \beta_2, \alpha_2$	

with

$$\alpha_1 = 0.05971588$$

$$\beta_1 = 0.47014206$$

$$\alpha_2 = 0.79742699$$

$$\beta_2 = 0.101286505$$

Note the error in the value of α_1 as given in reference 6, page 151.

APPENDIX E

STATIC CONDENSATION

The details of static condensation, by which the stiffness and load terms associated with the internal grid points of the quadrilateral are eliminated, are briefly described in this appendix.

Let the stiffness matrix $[K]_e$ and load vector $\{P\}_e$ of the quadrilateral element be partitioned with respect to grid points on the boundary (subscript b) and interior (subscript i) as follows:

$$[K]_e = \begin{bmatrix} k_{bb} & k_{bi} \\ k_{ib} & k_{ii} \end{bmatrix} \quad \{P\}_e = \begin{Bmatrix} P_b \\ P_i \end{Bmatrix} \quad (E1)$$

Let the total potential energy defined as a functional of the displacements be X . The finite element process is equivalent to an approximate minimization of the functional X with respect to grid point displacements. The total functional is equal to the sum of the contributions of all the elements; that is,

$$X = \sum_{e=1}^n X_e \quad (E2)$$

Let $\{\phi\}$ be the displacements of the quadrilateral element which will be subdivided into parts that are on the boundary (and hence common with other elements) $\{\phi\}_b$ and parts that occur in the particular element only $\{\phi\}_i$.

The finite element equations for any element can be written as

$$\frac{\partial X_e}{\partial \{\phi\}} = [K]_e \{\phi\}_e + \{P\}_e \quad (E3)$$

such that the matrix equation for the total structure is

$$[K]\{\phi\} + \{P\} = \{0\} \quad (E4)$$

APPENDIX E

where

$$[\mathbf{K}] = \sum_{e=1}^n [\mathbf{K}]_e \quad (\text{E5})$$

and

$$\{\mathbf{P}\} = \sum_{e=1}^n \{\mathbf{P}\}_e \quad (\text{E6})$$

with the summations being as in standard structural assembly process.

To minimize the functional X with respect to the displacements of the element $\{\phi\}$, a system of equations can be expressed by

$$\frac{\partial X}{\partial \{\phi\}} = 0 \quad (\text{E7})$$

By virtue of equation (E2), equation (E7) can also be written as

$$\sum_{e=1}^n \frac{\partial X_e}{\partial \{\phi\}} = 0 \quad (\text{E8})$$

Equation (E8) can be partitioned as

$$\sum_{e=1}^n \frac{\partial X_e}{\partial \{\phi\}_b} = 0 \quad (\text{E9})$$

$$\sum_{e=1}^n \frac{\partial X_e}{\partial \{\phi\}_i} = 0 \quad (\text{E10})$$

By noting that $\{\phi\}_i$ occurs only on the particular element, equation (E10) can be written as

APPENDIX E

$$\frac{\partial X_e}{\partial \{\phi\}_i} = 0 \quad (\text{E11})$$

for every element. Partitioning equation (E3) and using equations (E11) and (E1) yields

$$\frac{\partial X_e}{\partial \{\phi\}} = \begin{Bmatrix} \frac{\partial X_e}{\partial \{\phi\}_b} \\ 0 \end{Bmatrix} = \begin{bmatrix} k_{bb} & k_{bi} \\ k_{ib} & k_{ii} \end{bmatrix} \begin{Bmatrix} \{\phi\}_b \\ \{\phi\}_i \end{Bmatrix} + \begin{Bmatrix} \{P_b\} \\ \{P_i\} \end{Bmatrix} \quad (\text{E12})$$

From the second row of equation (E12), it can be written that

$$\{\phi\}_i = -[k_{ii}]^{-1} \left([k_{ib}] \{\phi\}_b + \{P_i\} \right) \quad (\text{E13})$$

which on substitution into the first set of equations yields

$$\frac{\partial X_e}{\partial \{\phi\}_b} = [K^*]_b \{\phi\}_b + \{P^*\}_b \quad (\text{E14})$$

where

$$[K^*]_b = [K^*]_e = [k_{bb}] - [k_{bi}] [k_{ii}]^{-1} [k_{ib}] \quad (\text{E15})$$

$$\{P^*\}_b = \{P^*\}_e = \{P_b\} - [k_{bi}] [k_{ii}]^{-1} \{P_i\} \quad (\text{E16})$$

The matrix equation for the total structure would still be given by equation (E4) so that

$$[K] = \sum_{e=1}^n [K^*]_e \quad (\text{E17})$$

$$\{P\} = \sum_{e=1}^n \{P^*\}_e \quad (\text{E18})$$

APPENDIX F

MEDIAN PLANE FOR QUADRILATERAL ELEMENT

The median plane is selected to be parallel to, and midway between, the diagonals of the quadrilateral. The calculations for establishing the median plane and the associated transformation matrix from global coordinates to in-plane coordinates are explained in this appendix.

The following equations are used to calculate the three unit vectors in the median plane $\{i\}$, $\{j\}$, and $\{k\}$ which define the element coordinate system (see fig. 3(c)):

$$\{V_i\} = \begin{Bmatrix} X_i \\ Y_i \\ Z_i \end{Bmatrix} \quad (i = 1, 2, \dots, 8) \quad (F1)$$

The diagonals are

$$\{d_1\} = \{V_8\} - \{V_1\} \quad (F2)$$

$$\{d_2\} = \{V_6\} - \{V_3\} \quad (F3)$$

$$\{k\} = \frac{\{d_1\} \times \{d_2\}}{|\{d_1\} \times \{d_2\}|} \quad (F4)$$

$$\{a_1\} = \{V_3\} - \{V_1\} \quad (F5)$$

$$\hat{h} = \frac{1}{2} \{a_1\}^T \{k\} \quad (F6)$$

The vectors lying in the median plane are computed from

$$\{i\} = \frac{\{a_1\} - 2\hat{h}\{k\}}{|\{a_1\} - 2\hat{h}\{k\}|} \quad (F7)$$

APPENDIX F

$$\{j\} = \{k\} \times \{i\} \tag{F8}$$

The transformation matrix from global coordinates to in-plane coordinates is, for the purposes of evaluation of the stiffness matrix,

$$\begin{Bmatrix} X'_1 \\ Y'_1 \\ Z'_1 \end{Bmatrix} = [\lambda] \begin{Bmatrix} X_1 \\ Y_1 \\ Z_1 \end{Bmatrix} \tag{F9}$$

where

$$[\lambda] = \begin{bmatrix} i_1 & i_2 & i_3 \\ j_1 & j_2 & j_3 \\ k_1 & k_2 & k_3 \end{bmatrix} \tag{F10}$$

and X'_1 , Y'_1 , and Z'_1 are the coordinates in the median plane.

APPENDIX G

REDUCTION OF MASS MATRIX FOR QUADRILATERAL ELEMENT IN DYNAMIC ANALYSIS

The equation for free vibrations of elastic structures vibrating at circular frequency ω can be written as

$$([\mathbf{K}] - \omega^2[\mathbf{M}])\{\Delta_0\} = 0 \quad (G1)$$

where $[\mathbf{K}]$ is the stiffness matrix, $[\mathbf{M}]$ is the mass matrix, and $\{\Delta_0\}$ is the vector of displacement amplitudes. This is a typical eigenvalue problem from which the natural frequencies of the system can be obtained.

The stiffness matrix $[\mathbf{K}]$ can be evaluated by using equations (E15) and (E17). The mass matrix of the quadrilateral element is obtained by adding the mass matrices of the constituent triangular elements and then eliminating the mass associated with the internal degrees of freedom by using the Guyan reduction scheme. Let the mass matrix of the element $[\mathbf{M}]_e$ be partitioned in terms of degrees of freedom at boundary (subscript b) and at interior (subscript i) as follows:

$$[\mathbf{M}]_e = \begin{bmatrix} m_{bb} & m_{bi} \\ m_{ib} & m_{ii} \end{bmatrix} \quad (G2)$$

From equation (E13), in the absence of any forces on interior points,

$$\{\phi\}_i = [\mathbf{G}_0]\{\phi\}_b \quad (G3)$$

where

$$[\mathbf{G}_0] = -[\mathbf{k}_{ii}]^{-1}[\mathbf{k}_{ib}] \quad (G4)$$

For cases with applied forces on the quadrilateral element, the reduced dynamic load vector is, by analogy to equation (E16),

APPENDIX G

$$\{P^*\}_b = \{P_b\} + [G_o]^T \{P_i\} \quad (G5)$$

By virtue of equation (G3), $\{\phi\}_e$ can be written as

$$\{\phi\}_e = \begin{Bmatrix} \{\phi\}_b \\ \{\phi\}_i \end{Bmatrix} = \begin{bmatrix} [I] \\ [G_o] \end{bmatrix} \{\phi\}_b \quad (G6)$$

that is,

$$\{\phi\}_e = [T_3] \{\phi\}_b \quad (G7)$$

where

$$[T_3] = \begin{bmatrix} [I] \\ [G_o] \end{bmatrix} \quad (G8)$$

and $[I]$ is the identity matrix.

The resulting mass matrix, referred to degrees of freedom at boundary grid points of the quadrilateral, is

$$\begin{aligned} [M^*]_e &= [T_3]^T [M]_e [T_3] \\ &= \begin{bmatrix} [I] & [G_o] \end{bmatrix}^T \begin{bmatrix} m_{bb} & m_{bi} \\ m_{ib} & m_{ii} \end{bmatrix} \begin{bmatrix} [I] \\ [G_o] \end{bmatrix} \\ &= [m_{bb}] + [G_o]^T [m_{ib}] + [m_{bi}] [G_o] + [G_o]^T [m_{ii}] [G_o] \end{aligned} \quad (G9)$$

APPENDIX G

The assembled mass matrix $[M]$ of the structure is

$$[M] = \sum_{e=1}^n [M^*]_e \quad (G10)$$

APPENDIX H

EFFECT OF POISSON'S RATIO ON FINITE ELEMENT APPROXIMATIONS

For the example problems considered in this report, namely, uniform plates subjected only to a normal load and having boundaries consisting entirely of segments that are either (a) clamped or (b) simply supported and straight, the differential equations as well as the boundary conditions are independent of Poisson's ratio and, hence, the exact solutions are also independent of Poisson's ratio. (An indirect dependence on ν through the plate rigidity D is not considered here for purposes of this discussion.) Cowper et al. (ref. 5) prove that this independence is true of finite element approximations provided the elements conform. For nonconforming elements, like the present elements, the finite element approximations are dependent on Poisson's ratio even for the aforementioned class of problems of plate bending. No data are presently available in the literature on the extent of this dependence. To study the effect of Poisson's ratio on the finite element approximations using the present elements, a numerical experiment was conducted on the static analysis of a square plate with clamped and simply supported edges. Twelve values of Poisson's ratio were used: 0.0, 0.05, 0.10, 0.166, 0.20, 0.25, 0.30, 0.333, 0.40, 0.45, 0.49, and 0.495. Due to symmetry, only one-fourth of the plate is analyzed. For completeness, the dimensions of the square plate and values of elastic modulus used are listed:

Length of side of plate, L , 1.2192 m (48 in.)

Thickness of plate, t , 0.0762 m (3 in.)

Elastic modulus, E , 4.788 GN/m² (6.944×10^5 psi)

For the mesh subdivision of $N = 2$ with the P arrangement (fig. 4(c)), the 18 eigenvalues of the 18×18 stiffness matrix of a triangular element for the 12 values of Poisson's ratio are shown in table H1. From the table, it is seen that although the largest eigenvalue (eigenvalue 1) changes with Poisson's ratio approximately as the plate rigidity

$D \left(D = \frac{Et^3}{12(1 - \nu^2)} \right)$, eigenvalues 2 to 15 do not clearly follow any specific trend. Eigenvalues 16, 17, and 18 are practically equal to zero and correspond to the rigid body modes.

Values of the coefficient for central deflection for different Poisson's ratios for simply supported and clamped plates for central concentrated loads and uniformly distributed loads are shown in tables H2 to H5. The results for Q mesh of simply supported plate and P mesh of clamped plate are plotted in figures H1 to H4. From tables H2 to H5 and figures H1 to H4, it is seen that the effect of an increase in the Poisson's ratio is to make the finite element approximation (using these elements) of the structure more

APPENDIX H

flexible. Also, it can be noted that the percentage error in the coefficients for simply supported plates for $\nu = 0.0$ even for coarse meshes is quite small and is comparable to that of the conforming elements of references 3, 4, and 5.

Values of the coefficient for central deflection for Poisson's ratio of 0.0 for the quadrilateral elements QUAD1 and QUAD5 are given in tables H6 and H7. As before, it is seen that the percentage error in the coefficients for $\nu = 0.0$ is quite small even for the coarsest mesh.

To study the effect of variation of Poisson's ratio on the vibration analysis, the non-dimensional eigenvalues were evaluated for $\nu = 0.0$ for mesh size of $N = 2$ and $N = 4$ for the simply supported and clamped square plates. The results are presented in tables H8 and H9. Again, it is observed that the percentage error in the lowest eigenvalue for the simply supported plate for $\nu = 0.0$ is very small even for the coarsest mesh.

APPENDIX H

TABLE H1.- EIGENVALUES OF STIFFNESS MATRIX FOR
VARIOUS POISSON'S RATIOS

Eigenvalue	$\nu = 0.0$	$\nu = 0.05$	$\nu = 0.10$	$\nu = 0.166$	$\nu = 0.20$	$\nu = 0.25$
1	1.3069E+07	1.3083E+07	1.3164E+07	1.3382E+07	1.3542E+07	1.3853E+07
2	9.5575E+06	9.5485E+06	9.5868E+06	9.7144E+06	9.8133E+06	1.0010E+07
3	6.1866E+06	6.1701E+06	6.1855E+06	6.2576E+06	6.3172E+06	6.4388E+06
4	3.6924E+06	3.7012E+06	3.7288E+06	3.7965E+06	3.8445E+06	3.9364E+06
5	2.1206E+06	2.1224E+06	2.1351E+06	2.1701E+06	2.1958E+06	2.2458E+06
6	1.2807E+06	1.2893E+06	1.3045E+06	1.3355E+06	1.3561E+06	1.3939E+06
7	4.7615E+05	4.7597E+05	4.7851E+05	4.8631E+05	4.9223E+05	5.0388E+05
8	3.5783E+05	3.4716E+05	3.3741E+05	3.2572E+05	3.2037E+05	3.1294E+05
9	2.1174E+05	2.0794E+05	2.0491E+05	2.0200E+05	2.0101E+05	2.0010E+05
10	1.4687E+05	1.4028E+05	1.3431E+05	1.2718E+05	1.2392E+05	1.1938E+05
11	1.1279E+05	1.1103E+05	1.0932E+05	1.0711E+05	1.0603E+05	1.0443E+05
12	6.6299E+04	6.3965E+04	6.1851E+04	5.9337E+04	5.8197E+04	5.6622E+04
13	6.3454E+04	6.1083E+04	5.8994E+04	5.6593E+04	5.5539E+04	5.4122E+04
14	3.8497E+04	3.7987E+04	3.7475E+04	3.6778E+04	3.6422E+04	3.5876E+04
15	2.9989E+04	2.9995E+04	2.9997E+04	2.9988E+04	2.9977E+04	2.9952E+04
16	-5.2898E-07	8.8311E-07	1.4591E-06	5.5643E-07	8.9640E-07	9.5491E-08
17	-7.2196E-07	-6.6216E-07	8.1557E-07	2.6894E-07	6.0835E-07	-4.5497E-07
18	-2.4895E-06	-3.2533E-06	-2.2123E-06	-2.0010E-06	-2.0421E-06	-9.9257E-07
Eigenvalue	$\nu = 0.30$	$\nu = 0.333$	$\nu = 0.40$	$\nu = 0.45$	$\nu = 0.49$	$\nu = 0.495$
1	1.4257E+07	1.4587E+07	1.5420E+07	1.6230E+07	1.7024E+07	1.7134E+07
2	1.0271E+07	1.0487E+07	1.1036E+07	1.1575E+07	1.2106E+07	1.2179E+07
3	6.6038E+06	6.7407E+06	7.0930E+06	7.4408E+06	7.7847E+06	7.8325E+06
4	4.0550E+06	4.1511E+06	4.3922E+06	4.6260E+06	4.8546E+06	4.8863E+06
5	2.3112E+06	2.3646E+06	2.4995E+06	2.6309E+06	2.7598E+06	2.7777E+06
6	1.4413E+06	1.4790E+06	1.5720E+06	1.6609E+06	1.7470E+06	1.7589E+06
7	5.1924E+05	5.3183E+05	5.6370E+05	5.9479E+05	6.2529E+05	6.2952E+05
8	3.0617E+05	3.0201E+05	2.9452E+05	2.8963E+05	2.8618E+05	2.8578E+05
9	1.9992E+05	2.0022E+05	2.0197E+05	2.0443E+05	2.0726E+05	2.0767E+05
10	1.1521E+05	1.1261E+05	1.0783E+05	1.0456E+05	1.0212E+05	1.0182E+05
11	1.0287E+05	1.0184E+05	9.9829E+04	9.8354E+04	9.7198E+04	9.7054E+04
12	5.5194E+04	5.4319E+04	5.2737E+04	5.1686E+04	5.0924E+04	5.0833E+04
13	5.2882E+04	5.2145E+04	5.0859E+04	5.0039E+04	4.9460E+04	4.9393E+04
14	3.5315E+04	3.4934E+04	3.4158E+04	3.3569E+04	3.3096E+04	3.3037E+04
15	2.9916E+04	2.9884E+04	2.9803E+04	2.9725E+04	2.9652E+04	2.9643E+04
16	4.2738E-07	3.4780E-07	1.8821E-06	6.2980E-07	1.1078E-06	1.7082E-06
17	6.2187E-08	-7.6369E-08	-5.6961E-07	-3.2935E-07	-1.9916E-07	-3.6222E-07
18	-1.7431E-06	-2.7652E-06	-3.8552E-06	-2.5545E-06	-1.8411E-06	-1.3526E-06

TABLE H2.- COEFFICIENT FOR CENTRAL DEFLECTION $\frac{1000 w_c D}{PL^2}$ DUE TO CENTRAL
CONCENTRATED LOAD P ON SIMPLY SUPPORTED PLATE

Poisson's ratio, ν	N = 2		N = 4		N = 6		N = 8		N = 12	
	Q Arrangement	P Arrangement	Q Arrangement	P Arrangement	Q Arrangement	P Arrangement	Q Arrangement	P Arrangement	Q Arrangement	P Arrangement
0.0	11.8270	12.0650	11.7661	11.7055	11.6901	11.6472	11.6564	11.6271	11.6285	11.6128
.05	11.9011	12.1349	11.7987	11.7202	11.7069	11.6534	11.6667	11.6306	11.6336	11.6143
.10	11.9870	12.2118	11.8368	11.7371	11.7265	11.6608	11.6787	11.6347	11.6396	11.6162
.166	12.1225	12.3266	11.8974	11.7638	11.7579	11.6728	11.6980	11.6416	11.6491	11.6193
.20	12.2003	12.3900	11.9325	11.7791	11.7761	11.6798	11.7092	11.6457	11.6547	11.6212
.25	12.3312	12.4938	11.9923	11.8048	11.8072	11.6917	11.7283	11.6527	11.6642	11.6245
.30	12.4810	12.6096	12.0618	11.8344	11.8434	11.7057	11.7506	11.6609	11.6753	11.6284
.333	12.5928	12.6943	12.1144	11.8564	11.8709	11.7162	11.7676	11.6671	11.6837	11.6314
.40	12.8494	12.8851	12.2377	11.9073	11.9356	11.7408	11.8076	11.6818	11.7036	11.6385
.45	13.0755	13.0504	12.3495	11.9524	11.9946	11.7629	11.8441	11.6951	11.7219	11.6449
.49	13.2810	13.1993	12.4538	11.9936	12.0479	11.7833	11.8784	11.7074	11.7390	11.6590
.495	13.3084	13.2191	12.4679	11.9992	12.0574	11.7860	11.8831	11.7091	11.7414	11.6518

TABLE H3.- COEFFICIENT FOR CENTRAL DEFLECTION $\frac{1000 w_c D}{qL^4}$ DUE TO UNIFORMLY
DISTRIBUTED LOAD q ON SIMPLY SUPPORTED PLATE

Poisson's ratio, ν	N = 2		N = 4		N = 6		N = 8		N = 12	
	Q Arrangement	P Arrangement	Q Arrangement	P Arrangement	Q Arrangement	P Arrangement	Q Arrangement	P Arrangement	Q Arrangement	P Arrangement
0.0	4.0807	4.1730	4.0666	4.0749	4.0642	4.0668	4.0634	4.0646	4.0628	4.0633
.05	4.0907	4.1843	4.0688	4.0758	4.0651	4.0671	4.0639	4.0648	4.0630	4.0633
.10	4.1042	4.1968	4.0719	4.0770	4.0663	4.0675	4.0645	4.0650	4.0633	4.0635
.166	4.1279	4.2154	4.0778	4.0793	4.0687	4.0684	4.0658	4.0655	4.0639	4.0637
.20	4.1426	4.2257	4.0816	4.0807	4.0703	4.0691	4.0667	4.0659	4.0643	4.0639
.25	4.1685	4.2428	4.0885	4.0833	4.0732	4.0702	4.0683	4.0666	4.0649	4.0642
.30	4.1996	4.2616	4.0972	4.0865	4.0769	4.0717	4.0703	4.0674	4.0658	4.0646
.333	4.2236	4.2754	4.1040	4.0890	4.0799	4.0729	4.0720	4.0681	4.0665	4.0649
.40	4.2806	4.3067	4.1208	4.0952	4.0872	4.0758	4.0760	4.0699	4.0683	4.0657
.45	4.3324	4.3339	4.1367	4.1009	4.0943	4.0786	4.0799	4.0715	4.0700	4.0665
.49	4.3804	4.3583	4.1519	4.1064	4.1011	4.0813	4.0838	4.0731	4.0717	4.0673
.495	4.3869	4.3616	4.1540	4.1071	4.1021	4.0817	4.0843	4.0734	4.0720	4.0674

TABLE H4. - COEFFICIENT FOR CENTRAL DEFLECTION $\frac{1000 w_c D}{PL^2}$ DUE TO CENTRAL
CONCENTRATED LOAD P ON CLAMPED PLATE

Poisson's ratio, ν	N = 2		N = 4		N = 6		N = 8		N = 12	
	Q Arrangement	P Arrangement	Q Arrangement	P Arrangement	Q Arrangement	P Arrangement	Q Arrangement	P Arrangement	Q Arrangement	P Arrangement
0.0	6.4089	6.1942	5.8213	5.6916	5.7214	5.6494	5.6794	5.6341	5.6452	5.6225
.05	6.4942	6.2705	5.8562	5.7089	5.7395	5.6571	5.6904	5.6384	5.6506	5.6244
.10	6.5878	6.3549	5.8957	5.7290	5.7601	5.6662	5.7030	5.6436	5.6568	5.6267
.166	6.7268	6.4812	5.9566	5.7605	5.7923	5.6808	5.7229	5.6520	5.6667	5.6306
.20	6.8034	6.5510	5.9911	5.7785	5.8107	5.6893	5.7342	5.6570	5.6723	5.6330
.25	6.9281	6.6651	6.0486	5.8087	5.8416	5.7037	5.7354	5.6655	5.6819	5.6370
.30	7.0662	6.7917	6.1141	5.8432	5.8772	5.7204	5.7756	5.6755	5.6930	5.6418
.333	7.1668	6.8839	6.1629	5.8688	5.9039	5.7330	5.7923	5.6831	5.7014	5.6454
.40	7.3916	7.0896	6.2751	5.9275	5.9660	5.7622	5.8314	5.7007	5.7211	5.6540
.45	7.5844	7.2654	6.3747	5.9790	6.0218	5.7881	5.8666	5.7166	5.7389	5.6619
.49	7.7563	7.4216	6.4661	6.0257	6.0735	5.8119	5.8995	5.7312	5.7557	5.6692
.495	7.7791	7.4422	6.4784	6.0319	6.0805	5.8151	5.9040	5.7332	5.7579	5.6701

TABLE H5. - COEFFICIENT FOR CENTRAL DEFLECTION $\frac{1000 w_c D}{qL^4}$ DUE TO UNIFORMLY
DISTRIBUTED LOAD q ON CLAMPED PLATE

Poisson's ratio, ν	N = 2		N = 4		N = 6		N = 8		N = 12	
	Q Arrangement	P Arrangement	Q Arrangement	P Arrangement	Q Arrangement	P Arrangement	Q Arrangement	P Arrangement	Q Arrangement	P Arrangement
0.0	1.4351	1.4206	1.2882	1.2738	1.2763	1.2683	1.2719	1.2670	1.2684	1.2661
.05	1.4544	1.4334	1.2922	1.2758	1.2779	1.2692	1.2727	1.2675	1.2688	1.2663
.10	1.4757	1.4477	1.2967	1.2783	1.2797	1.2704	1.2737	1.2682	1.2692	1.2667
.166	1.5073	1.4696	1.3039	1.2826	1.2827	1.2725	1.2753	1.2695	1.2699	1.2673
.20	1.5248	1.4819	1.3080	1.2851	1.2845	1.2738	1.2763	1.2702	1.2703	1.2676
.25	1.5533	1.5021	1.3149	1.2895	1.2874	1.2760	1.2780	1.2715	1.2711	1.2683
.30	1.5850	1.5249	1.3228	1.2946	1.2909	1.2786	1.2799	1.2731	1.2719	1.2690
.333	1.6081	1.5415	1.3288	1.2985	1.2936	1.2806	1.2814	1.2744	1.2726	1.2696
.40	1.6598	1.5791	1.3425	1.3075	1.2998	1.2853	1.2850	1.2773	1.2742	1.2711
.45	1.7043	1.6115	1.3548	1.3115	1.3055	1.2897	1.2882	1.2800	1.2757	1.2725
.49	1.7441	1.6404	1.3660	1.3228	1.3108	1.2936	1.2913	1.2826	1.2771	1.2737
.495	1.7493	1.6442	1.3675	1.3238	1.3115	1.2942	1.2917	1.2829	1.2773	1.2739

APPENDIX H

TABLE H6.- COEFFICIENTS FOR CENTRAL DEFLECTION OF SIMPLY
SUPPORTED SQUARE PLATE OF SIDE L FOR $\nu = 0.0$
FOR QUADRILATERAL ELEMENTS

Number of elements per side, N	Coefficient $\alpha = \frac{1000 w_c D}{PL^2}$ due to central concentrated load P		Coefficient $\beta = \frac{1000 w_c D}{qL^4}$ due to uniformly distributed load q	
	QUAD1	QUAD5	QUAD1	QUAD5
2	11.886797	12.294189	4.115169	4.177057
4	11.704203	11.760712	4.068629	4.078833
6	11.653533	11.673154	4.064797	4.068828
8	11.632881	11.642431	4.063666	4.065832
12	11.616516	11.620020	4.062927	4.063869
Exact	11.600		4.062	

TABLE H7.- COEFFICIENTS FOR CENTRAL DEFLECTION OF CLAMPED
SQUARE PLATE OF SIDE L FOR $\nu = 0.0$
FOR QUADRILATERAL ELEMENTS

Number of elements per side, N	Coefficient $\alpha = \frac{1000 w_c D}{PL^2}$ due to central concentrated load P		Coefficient $\beta = \frac{1000 w_c D}{qL^4}$ due to uniformly distributed load q	
	QUAD1	QUAD5	QUAD1	QUAD5
2	6.276204	6.634375	1.427327	1.499818
4	5.728607	5.774994	1.279252	1.286955
6	5.670867	5.683594	1.271472	1.270605
8	5.647926	5.652885	1.268923	1.267993
12	5.629617	5.630804	1.267001	1.266436
Exact	5.600		1.260	

TABLE H8.- NONDIMENSIONAL EIGENVALUES OF SIMPLY SUPPORTED SQUARE PLATE FOR $\nu = 0.0$

Mode (r,s)	N = 2				N = 4				Exact solution
	Triangular element		Quadrilateral element		Triangular element		Quadrilateral element		
	Q Arrangement	P Arrangement	QUAD1	QUAD5	Q Arrangement	P Arrangement	QUAD1	QUAD5	
(1,1)	386.14	384.97	388.10	387.20	388.93	388.74	389.08	388.53	389.64
(1,2)	2 477.59	2 477.59	2 558.41	2 628.19	2 415.26	2 415.26	2 420.91	2 427.66	2 435.23
(2,2)	6 541.93	6 541.94	7 997.35	8 910.19	6 179.56	6 179.56	6 209.53	6 195.16	6 234.18
(1,3)	7 149.37	10 008.09	10 116.30	10 413.34	9 482.08	9 334.84	9 620.47	9 769.04	9 740.91
	9 922.22	10 458.52	10 201.76	11 160.88	9 704.72	9 548.69	9 620.47	9 769.04	
(2,3)	18 181.25	18 181.25	22 162.54	25 570.30	16 144.46	16 144.46	16 358.12	16 436.21	16 462.14
(3,3)	32 072.08	35 119.77	39 554.70	46 018.82	30 843.18	30 676.12	31 361.90	31 498.11	31 560.55

TABLE H9.- NONDIMENSIONAL EIGENVALUES OF CLAMPED SQUARE PLATE FOR $\nu = 0.0$

Mode (r,s)	N = 2				N = 4				Upper bound (ref. 5)	Lower bound (ref. 5)
	Triangular element		Quadrilateral element		Triangular element		Quadrilateral element			
	Q Arrangement	P Arrangement	QUAD1	QUAD5	Q Arrangement	P Arrangement	QUAD1	QUAD5		
(1,1)	1 128.01	1 176.20	1 163.36	1 132.04	1 270.30	1 286.59	1 280.74	1 282.36	1 294.96	1 294.93
(1,2)	5 527.46	6 430.53	5 569.76	5 618.99	5 638.97	5 662.55	5 685.23	5 767.57	5 386.66	5 386.42
* (2,2)	-----	-----	-----	-----	11 813.51	11 938.64	11 972.76	11 821.41	11 710.83	11 709.96
(1,3)	16 022.77	18 218.73	17 835.65	17 162.29	16 290.10	16 028.25	16 534.90	17 013.24	17 313.50	17 311.47
(3,1)	16 316.84	18 492.14	22 112.03	21 159.71	16 615.87	16 390.92	16 576.13	17 082.72	17 478.13	17 475.96
* (2,3)	-----	-----	-----	-----	25 272.33	25 633.44	25 762.75	25 460.70	27 225.20	27 194.90
* (3,3)	-----	-----	-----	-----	42 967.97	42 377.02	43 813.12	42 606.72	48 414.60	48 368.80

*Values for N = 2 are quite high because of the small number of net degrees of freedom for analysis and, hence, are not recorded.

APPENDIX H

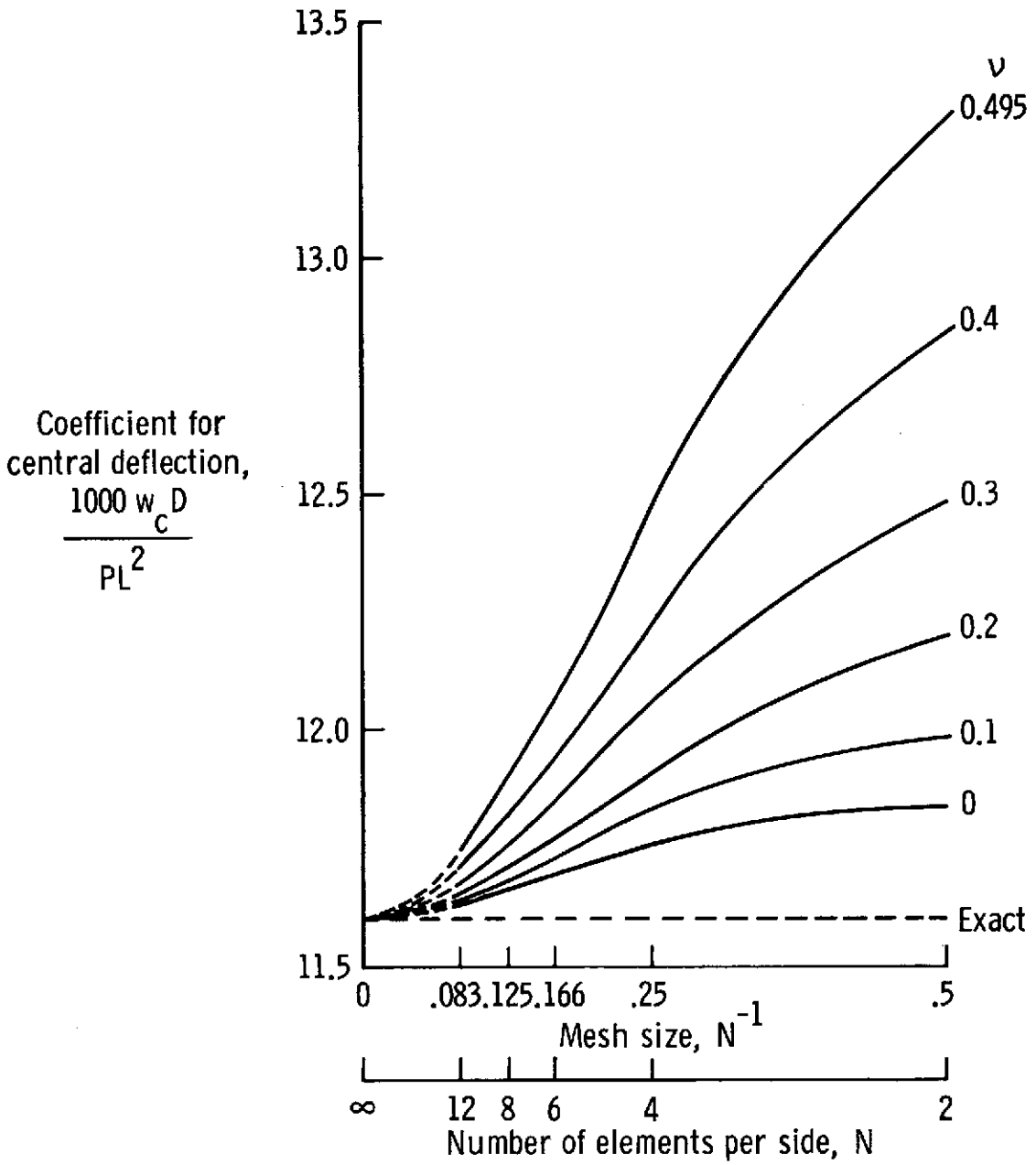


Figure H1.- Central concentrated load P on Q mesh of simply supported plate.

APPENDIX H

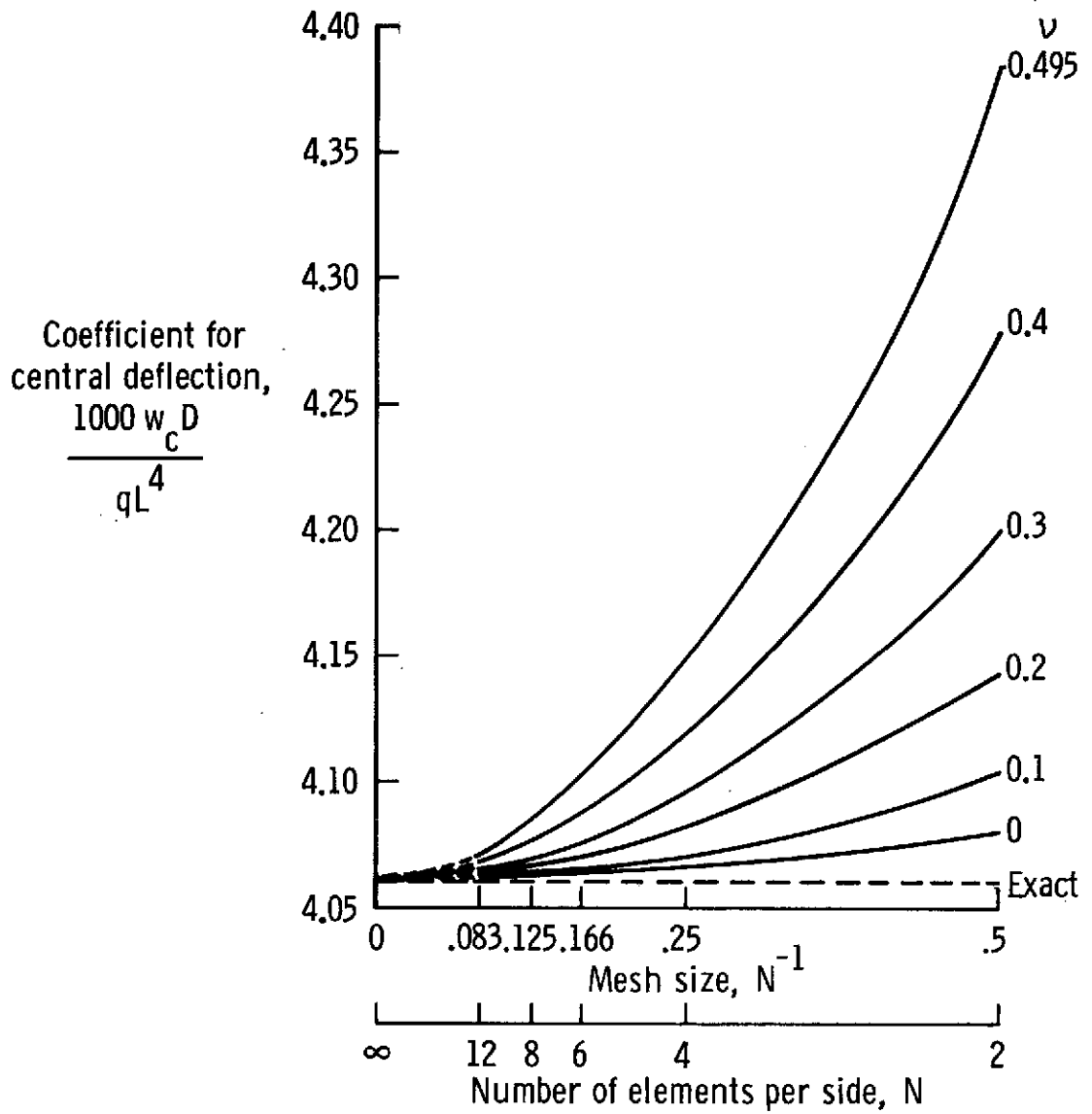


Figure H2.- Uniformly distributed load q on Q mesh of simply supported plate.

APPENDIX H

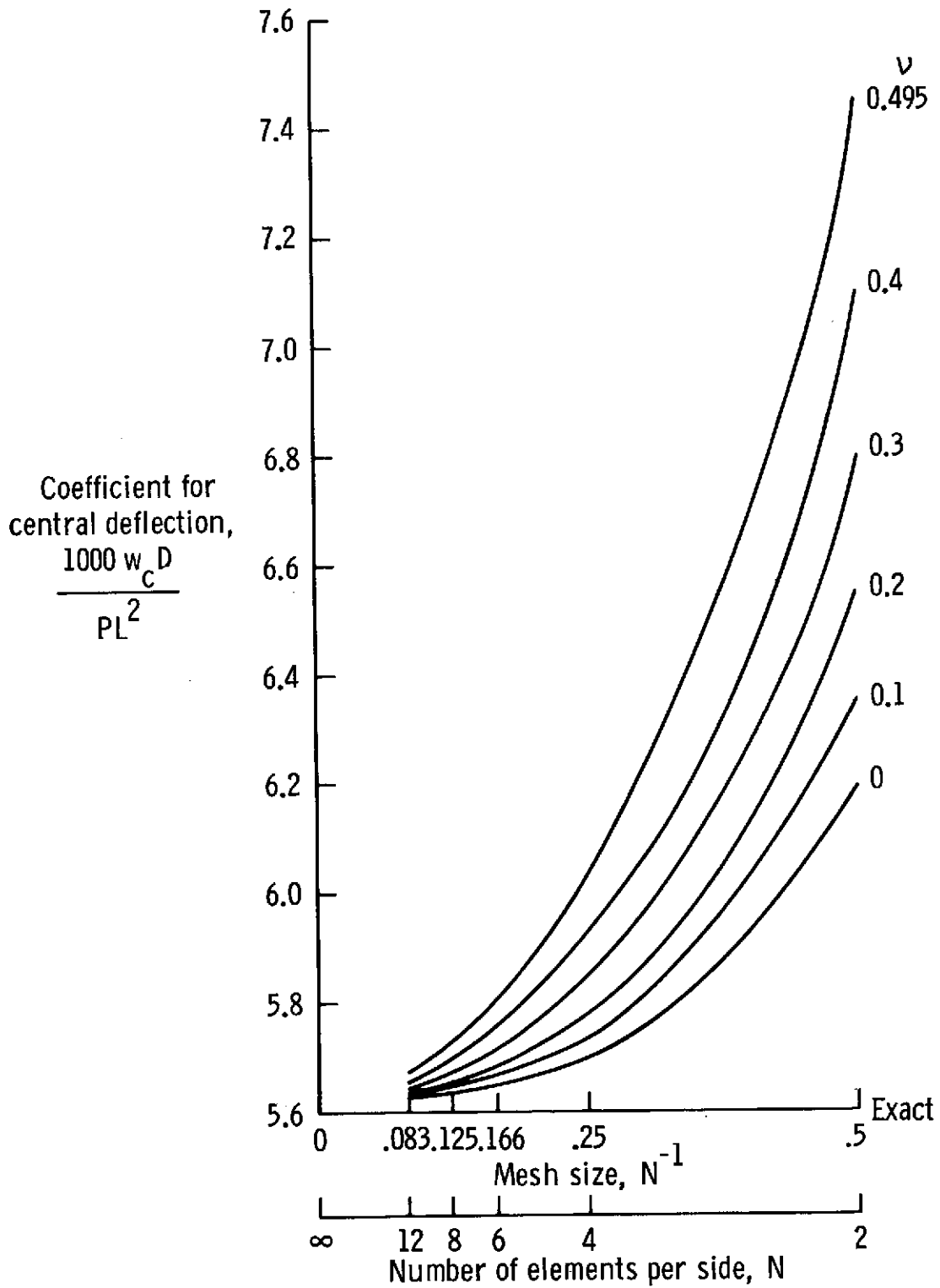


Figure H3.- Central concentrated load P on P mesh of clamped plate.

APPENDIX H

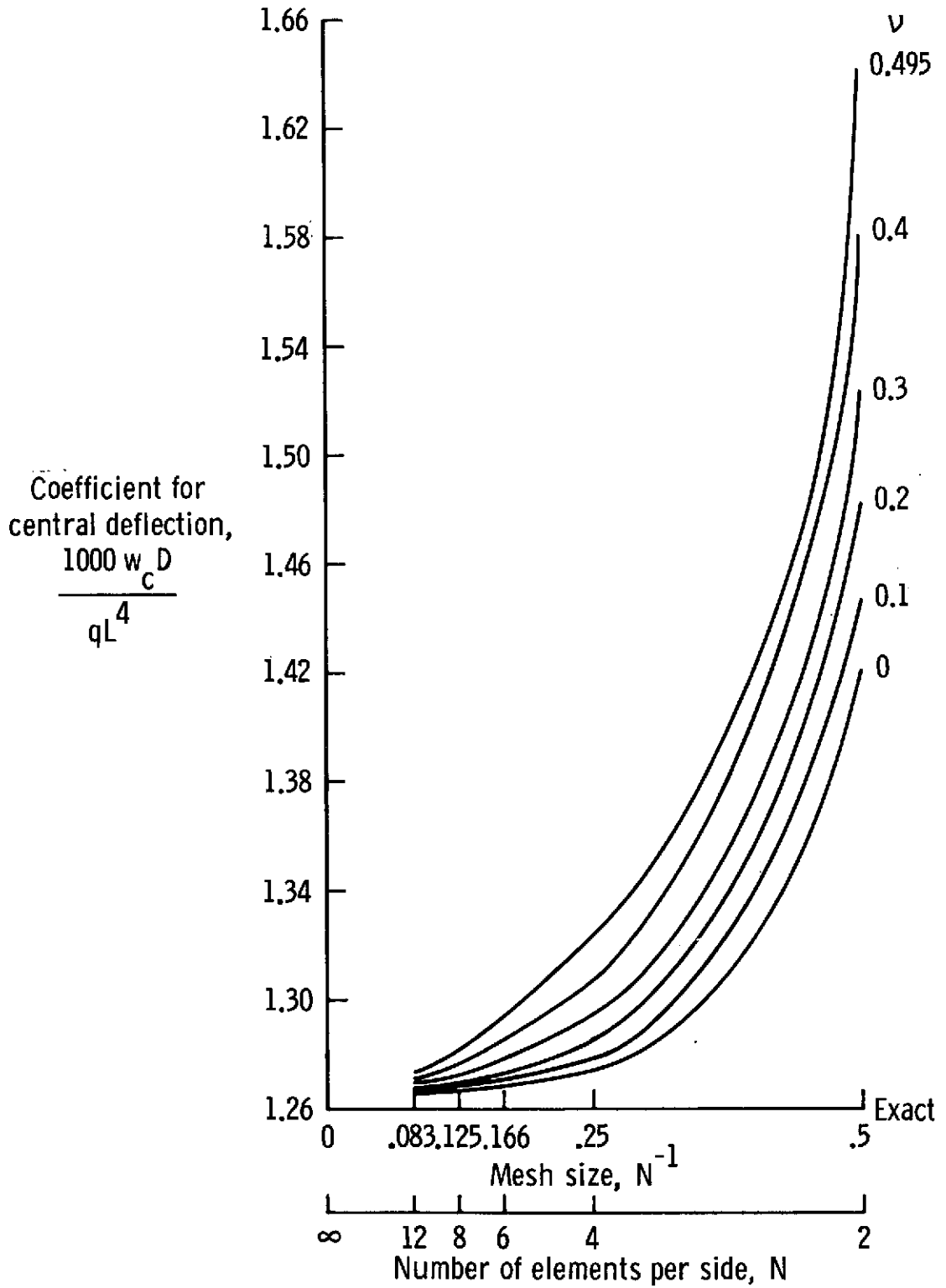


Figure H4.- Uniformly distributed load q on P mesh of clamped plate.

REFERENCES

1. Clough, Ray W.; and Tocher, James L.: Finite Element Stiffness Matrices for Analysis of Plate Bending. Matrix Methods in Structural Mechanics, AFFDL-TR-66-80, U.S. Air Force, [1965], pp. 515-545. (Available from DDC as AD 646 300.)
2. Bazeley, G. R.; Cheung, Y. K.; Irons, B. M.; and Zienkiewicz, O. C.: Triangular Elements in Plate Bending – Conforming and Non-Conforming Solutions. Matrix Methods in Structural Mechanics, AFFDL-TR-66-80, U.S. Air Force, Nov. 1966, pp. 547-576. (Available from DDC as AD 646 300.)
3. Argyris, J. H.; Buck, K. E.; Scharpf, D. W.; Hilber, H. M.; and Mareczek, G.: Some New Elements for the Matrix Displacement Method. Proceedings of the Second Conference on Matrix Methods in Structural Mechanics, AFFDL-TR-68-150, U.S. Air Force, Dec. 1969, pp. 333-397. (Available from DDC as AD 703 685.)
4. Bell, K.: Triangular Plate Bending Elements. Finite Element Methods in Stress Analysis, Ivar Holand and Kolbein Bell, eds., TAPIR (Trondheim, Norway), 1969, pp. 213-252.
5. Cowper, G. R.; Kosko, E.; Lindberg, G. M.; and Olson, M. D.: A High Precision Triangular Plate-Bending Element. Aeronaut. Rep. LR-514, Nat. Res. Council. Can. (Ottawa), Dec. 1968.
6. Zienkiewicz, O. C.: The Finite Element Method in Engineering Science. McGraw-Hill Book Co., Inc., c.1971.
7. MacNeal, Richard H., ed.: The NASTRAN Theoretical Manual (Level 15). NASA SP-221(01), 1972.
8. Timoshenko, S.; and Woinowsky-Krieger, S.: Theory of Plates and Shells. Second ed., McGraw-Hill Book Co., Inc., 1959.
9. Bell, Kolbein: A Refined Triangular Plate Bending Finite Element. Int. J. Numerical Methods Eng., vol. 1, no. 1, Jan.-Mar. 1969, pp. 101-122.
10. Clough, Ray W.; and Felippa, Carlos A.: A Refined Quadrilateral Element for Analysis of Plate Bending. Proceedings of the Second Conference on Matrix Methods in Structural Mechanics, AFFDL-TR-68-150, U.S. Air Force, Dec. 1969, pp. 399-440. (Available from DDC as AD 703 685.)

TABLE I.- CENTRAL DEFLECTION OF SIMPLY SUPPORTED SQUARE PLATE

Number of elements per side, N	Central concentrated load				Uniformly distributed load			
	Triangular element		Quadrilateral element		Triangular element		Quadrilateral element	
	Q Arrangement	P Arrangement	QUAD1	QUAD5	Q Arrangement	P Arrangement	QUAD1	QUAD5
2	12.481019	12.609566	12.415948	12.969755	4.199645	4.261581	4.206310	4.281619
4	12.061776	11.834372	11.867523	11.930068	4.097157	4.086519	4.084618	4.094603
6	11.843386	11.705700	11.733735	11.751625	4.076928	4.071701	4.071428	4.075169
8	11.750629	11.660884	11.681019	11.687980	4.070332	4.067423	4.067305	4.069277
12	11.675284	11.628410	11.661173	11.664712	4.065832	4.064577	4.066784	4.067732
Exact solution (ref. 8)	11.600				4.062			

TABLE II.- CENTRAL DEFLECTION OF CLAMPED SQUARE PLATE

Number of elements per side, N	Central concentrated load				Uniformly distributed load			
	Triangular element		Quadrilateral element		Triangular element		Quadrilateral element	
	Q Arrangement	P Arrangement	QUAD1	QUAD5	Q Arrangement	P Arrangement	QUAD1	QUAD5
2	7.066235	6.791689	6.836933	7.349924	1.584978	1.524858	1.542626	1.628655
4	6.114092	5.843160	5.901673	5.945223	1.322830	1.294588	1.301405	1.296453
6	5.877212	5.720419	5.757109	5.761662	1.290939	1.278577	1.281229	1.276015
8	5.775625	5.675495	5.699818	5.698141	1.279936	1.273145	1.274434	1.270888
12	5.693018	5.641786	5.677693	5.676650	1.271947	1.269034	1.272375	1.270499
Exact solution (ref. 8)	5.60				1.26			

TABLE III.- COEFFICIENTS OF CENTRAL DEFLECTION OF SQUARE PLATE INCLUDING TRANSVERSE SHEAR EFFECTS, USING TRIANGULAR ELEMENTS

$$[E = 4.788 \text{ GN/m}^2; \nu = 0.0; L/t = 96]$$

N	Mesh	Simply supported edges						Clamped edges					
		Central concentrated load P			Uniformly distributed load q			Central concentrated load P			Uniformly distributed load q		
		a	b	c	a	b	c	a	b	c	a	b	c
12	Q	11.628511	11.643453	0.1281%	4.062843	4.064213	0.0337%	5.645222	5.660855	0.2772%	1.268392	1.270035	0.1293%
12	P	11.612820	11.626107	0.1138%	4.063288	4.064431	0.0283%	5.622482	5.637223	0.2632%	1.266093	1.267783	0.1335%
		a Coefficient for central deflection without transverse shear effects						$\frac{1000 w_c D}{PL^2}$ for concentrated load P.					
		b Coefficient for central deflection with transverse shear effects						$\frac{1000 w_c D}{qL^4}$ for uniformly distributed load q.					
		c Increase in the coefficient due to transverse shear = $\frac{b-a}{a} \times 100$.											

TABLE IV.- NONDIMENSIONAL EIGENVALUES OF SIMPLY SUPPORTED SQUARE PLATE

$$\left[\lambda = \frac{\rho t \omega^2 L^4}{D} \right]$$

Mode (r,s)	N = 2				N = 4				Exact solution
	Triangular element		Quadrilateral element		Triangular element		Quadrilateral element		
	Q Arrangement	P Arrangement	QUAD1	QUAD5	Q Arrangement	P Arrangement	QUAD1	QUAD5	
(1,1)	378.95	380.13	382.46	380.65	386.89	387.47	387.65	387.12	389.64
(1,2)	2 476.96	2 476.96	2 579.27	2 614.69	2 386.91	2 386.91	2 393.62	2 408.43	2 435.23
(2,2)	6 541.94	6 541.94	7 997.35	8 943.58	6 090.60	6 090.60	6 119.33	6 090.40	6 234.18
(1,3)	7 361.34	9 154.84	9 278.13	9 890.04	9 060.72	8 952.28	9 375.75	9 635.83	9 740.91
	9 967.93	9 702.58	9 845.21	10 512.26	9 499.83	9 395.30	9 375.75	9 635.83	
(2,3)	17 713.33	17 713.33	20 601.13	25 672.94	15 670.75	15 670.75	15 917.84	15 980.11	16 462.14
(3,3)	29 521.72	32 609.40	36 340.21	44 996.98	29 507.27	29 477.98	30 132.14	29 981.26	31 560.55

TABLE V.- FINITE ELEMENT SOLUTIONS FOR LOWEST EIGENVALUE
OF SIMPLY SUPPORTED PLATE

Number of elements per side, N	ACM (ref. 1)	CFQ (ref. 10)	C-N (ref. 5)	Present elements			
				Triangular Q Arrangement	Triangular P Arrangement	QUAD1	QUAD5
2	324.77	-----	389.83	378.95	380.13	382.46	380.65
4	366.72	401.81	389.64	386.89	387.47	387.65	387.12
Exact solution	389.636						

TABLE VI.- NONDIMENSIONAL EIGENVALUES OF CLAMPED SQUARE PLATE

$$\left[\lambda = \frac{\rho t \omega^2 L^4}{D} \right]$$

Mode (r,s)	N = 2				N = 4				Upper bound (ref. 5)	Lower bound (ref. 5)
	Triangular element		Quadrilateral element		Triangular element		Quadrilateral element			
	Q Arrangement	P Arrangement	QUAD1	QUAD5	Q Arrangement	P Arrangement	QUAD1	QUAD5		
(1,1)	1 018.04	1 116.50	1 079.38	1 053.79	1 242.27	1 264.92	1 258.80	1 269.38	1 294.96	1 294.93
(1,2)	5 483.54	6 314.05	5 422.86	5 470.79	5 378.97	5 433.94	5 447.74	5 641.15	5 386.66	5 386.42
* (2,2)	-----	-----	-----	-----	11 186.95	11 403.98	11 387.93	11 313.97	11 710.83	11 709.96
(1,3)	16 011.69	17 837.24	17 948.30	17 150.06	14 895.44	14 783.07	15 517.61	16 494.60	17 313.50	17 311.47
(3,1)	16 160.85	18 399.41	21 599.55	21 159.71	15 656.77	15 620.66	15 556.55	16 548.29	17 478.13	17 475.96
* (2,3)	-----	-----	-----	-----	23 413.41	24 018.08	24 031.44	23 854.86	27 225.20	27 194.90
* (3,3)	-----	-----	-----	-----	38 928.26	39 976.01	40 121.98	38 417.69	48 414.60	48 368.80

*Values for N = 2 are quite high because of the small number of net degrees of freedom for analysis and, hence, are not recorded.

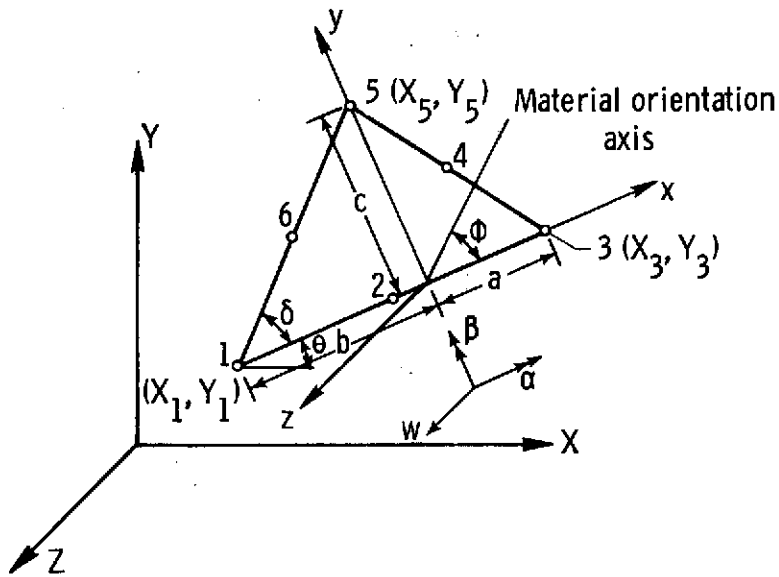


Figure 1.- Triangular element geometry.

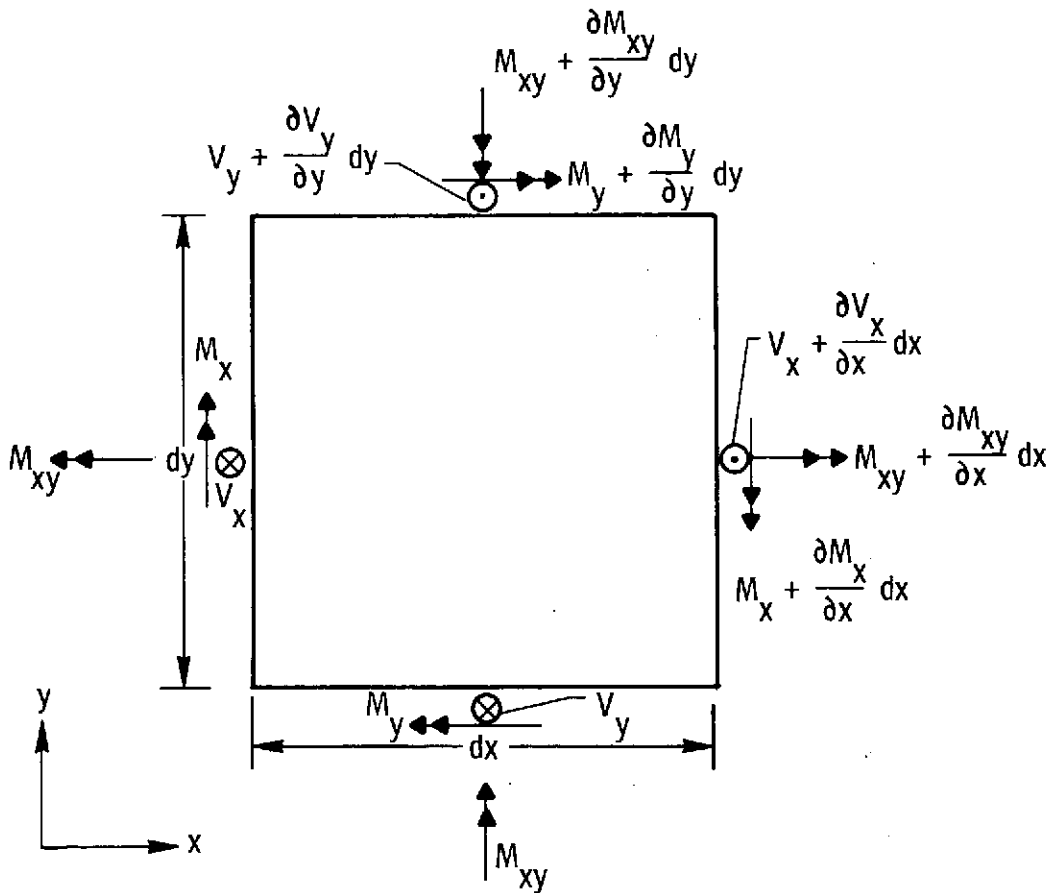
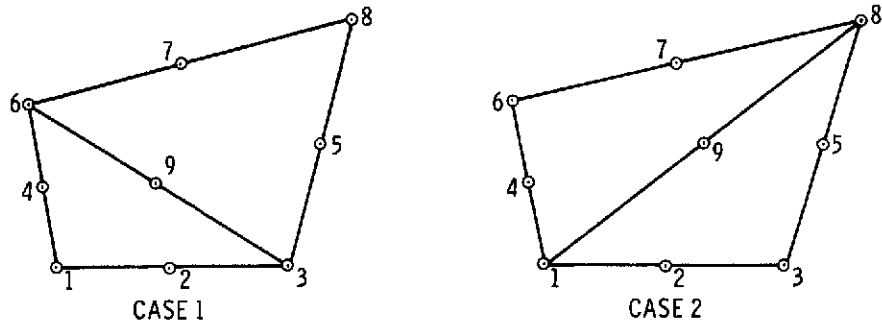
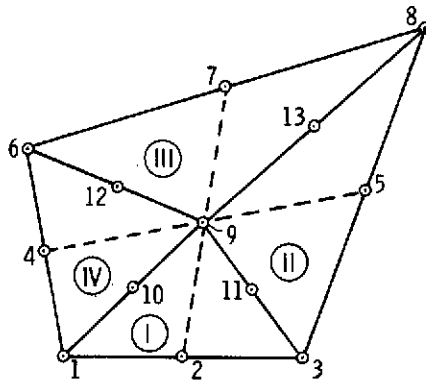


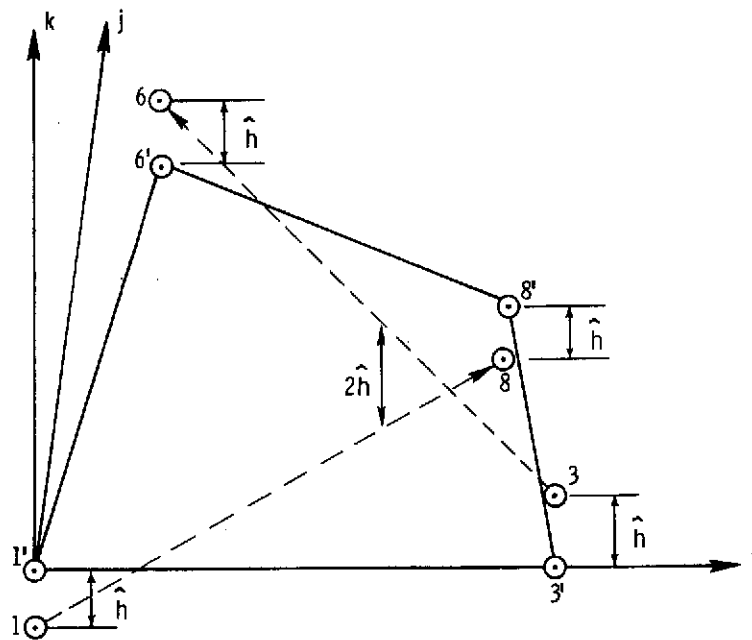
Figure 2.- Sign convention for moments and shears.



(a) QUAD1.

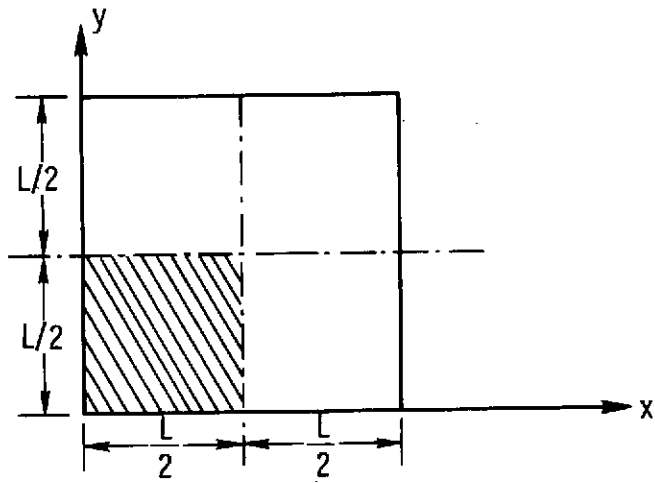


(b) QUAD5.

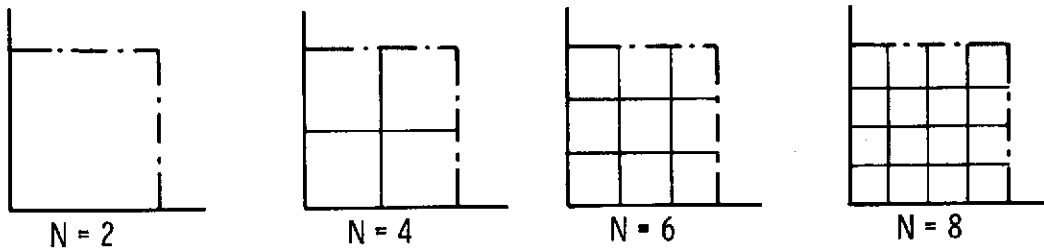


(c) Median plane for quadrilateral element.

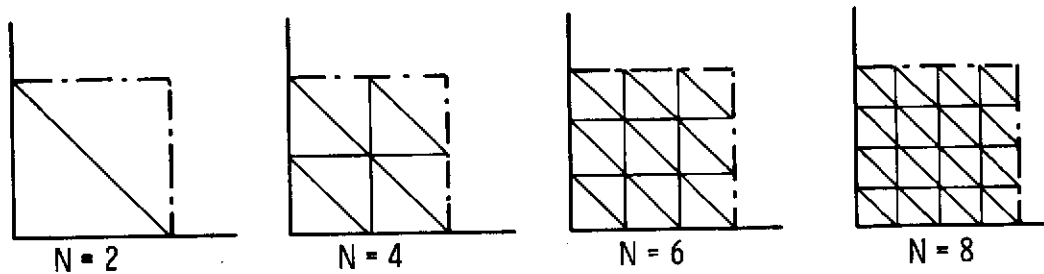
Figure 3.- Quadrilateral element geometry.



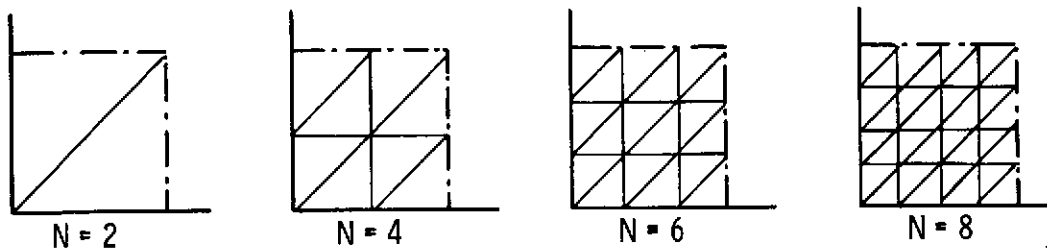
(a) Square plate of uniform thickness.



(b) Quadrilateral element mesh idealization.

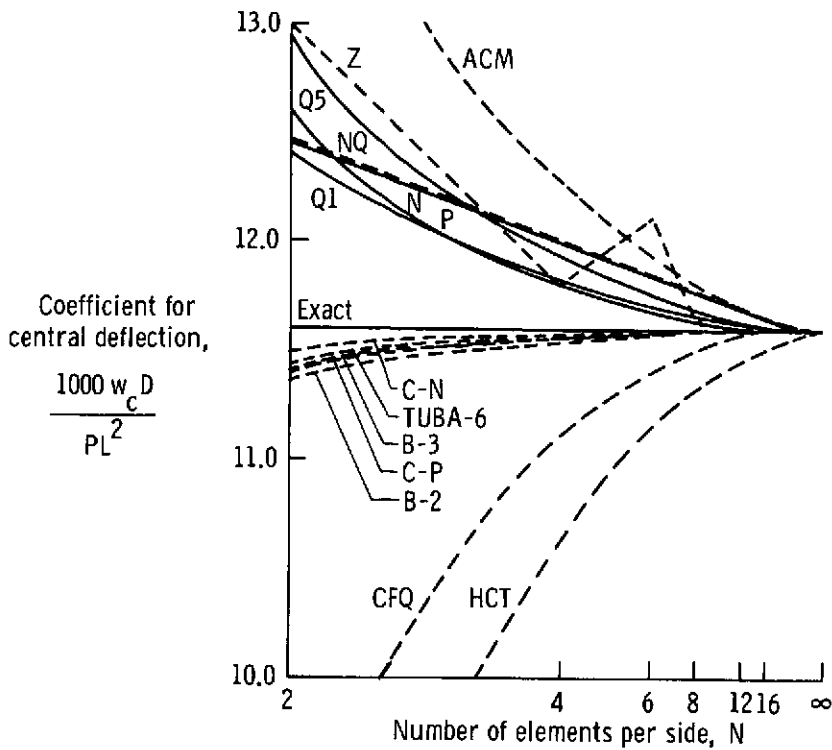


(c) P arrangement of triangular element mesh idealization.



(d) Q arrangement of triangular element mesh idealization.

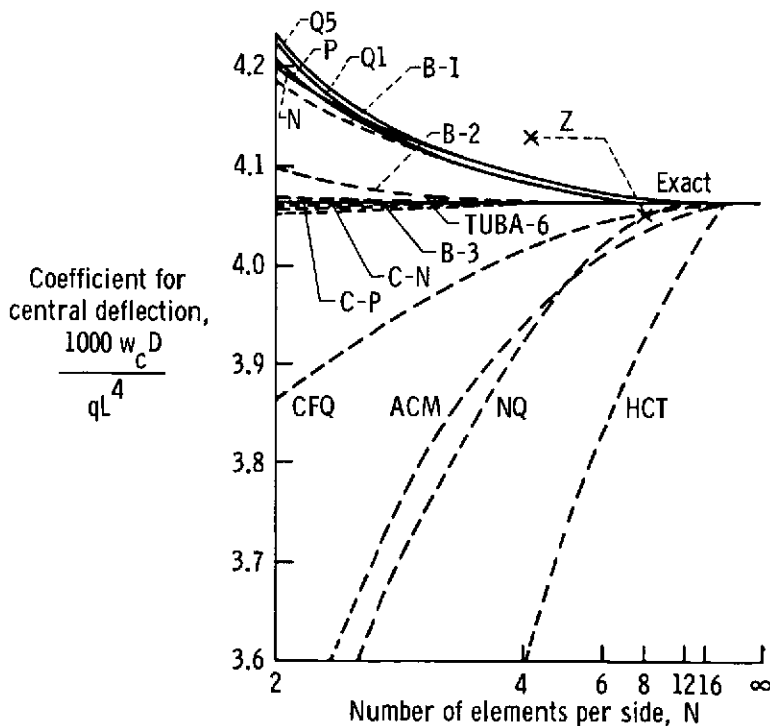
Figure 4.- Finite element idealization of square plate.



Notation	Element shape	Reference
N	T (Q mesh)	Present paper
P	T (P mesh)	Present paper
Q1	Q	Present paper
Q5	Q	Present paper
ACM	R	1
HCT	T	1
Z	T	2
TUBA-6	T	3
B-2	T (T-18)	4,9
B-3	T (T-21)	4,9
C-N	T (Q mesh)	5
C-P	T (P mesh)	5
NQ	Q	7
CFQ	Q	10

T - Triangular; Q - Quadrilateral; R - Rectangular

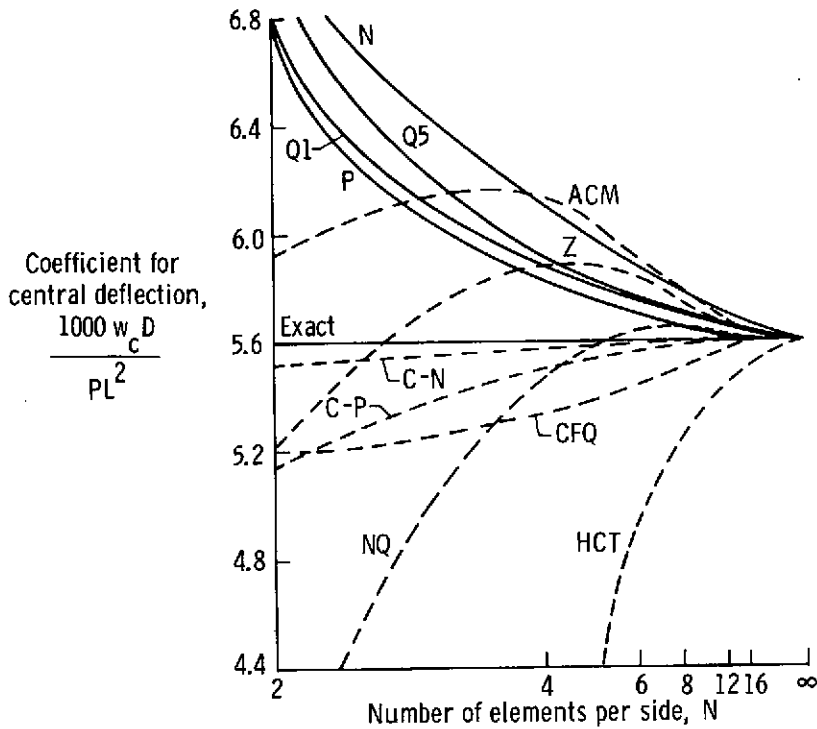
Figure 5.- Central deflection w_c due to central point load P on simply supported square plate.



Notation	Element shape	Reference
N	T (Q mesh)	Present paper
P	T (P mesh)	Present paper
Q1	Q	Present paper
Q5	Q	Present paper
ACM	R	1
HCT	T	1
Z	T	2
TUBA-6	T	3
B-1	T (T-15)	4
B-2	T (T-18)	4,9
B-3	T (T-21)	4,9
C-N	T (Q mesh)	5
C-P	T (P mesh)	5
NQ	Q	7
CFQ	Q	10

T - Triangular; Q - Quadrilateral; R - Rectangular

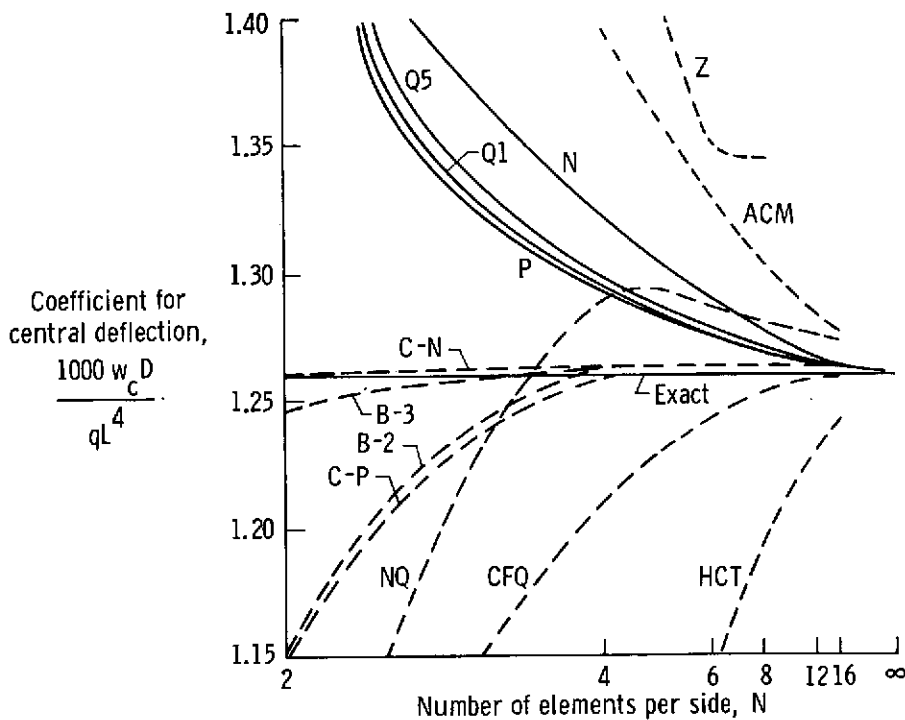
Figure 6.- Central deflection w_c due to uniformly distributed load q on simply supported square plate.



Notation	Element shape	Reference
N	T (Q mesh)	Present paper
P	T (P mesh)	Present paper
Q1	Q	Present paper
Q5	Q	Present paper
ACM	R	1
HCT	T	1
Z	T	2
C-N	T (Q mesh)	5
C-P	T (P mesh)	5
NQ	Q	7
CFQ	Q	10

T - Triangular; Q - Quadrilateral;
R - Rectangular

Figure 7.- Central deflection w_c due to central point load P on clamped square plate.



Notation	Element shape	Reference
N	T (Q mesh)	Present paper
P	T (P mesh)	Present paper
Q1	Q	Present paper
Q5	Q	Present paper
ACM	R	1
HCT	T	1
Z	T	2
B-2	T (T-18)	4,9
B-3	T (T-21)	4,9
C-N	T (Q mesh)	5
C-P	T (P mesh)	5
NQ	Q	7
CFQ	Q	10

T - Triangular; Q - Quadrilateral;
R - Rectangular

Figure 8.- Central deflection w_c due to uniformly distributed load q on clamped square plate.

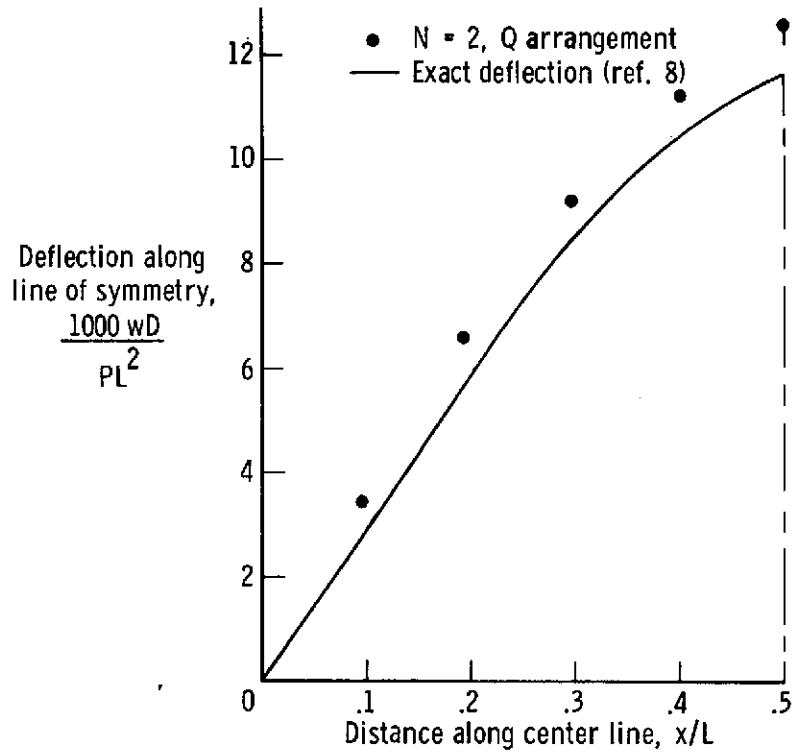


Figure 9.- Deflections along line of symmetry for simply supported plate due to central point load.

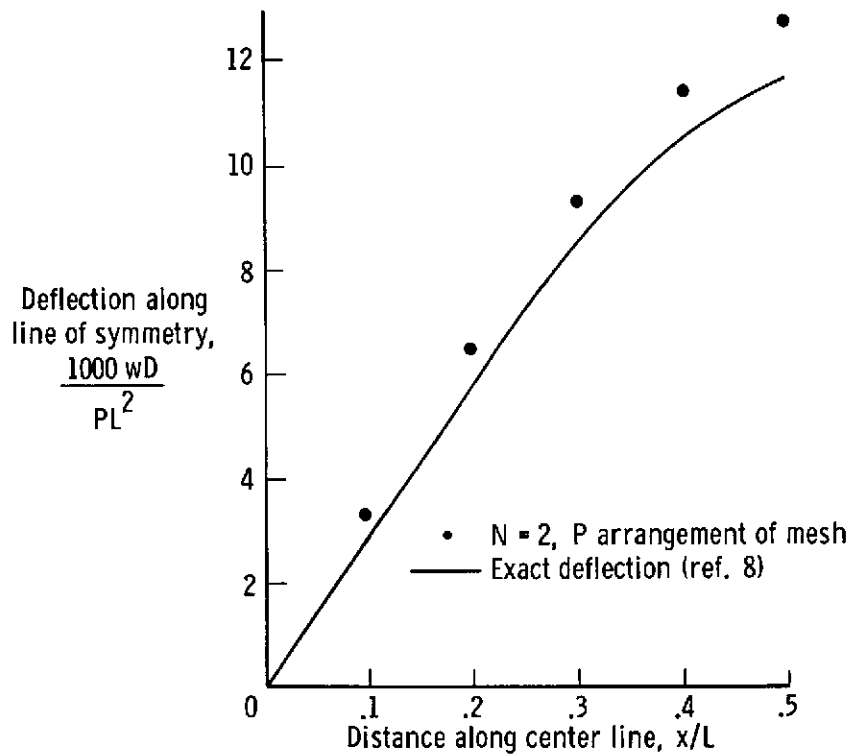


Figure 9.- Concluded.